EFFECT OF PROCESSING CONDITIONS ON THE SCRATCH AND MAR BEHAVIOR OF TPO SYSTEMS

A Thesis

by

MUKUND SHASTRY GUNDI

Submitted to the Office of Graduate and Professional Studies of
Texas A&M University
in partial fulfillment of the requirements for the degree of

MASTER OF SCIENCE

Chair of Committee,	Hung-Jue Sue
Committee Members,	Hong Liang
	Xiaofeng Qian
Head of Department,	Daniel McAdams

May 2016

Major Subject: Mechanical Engineering

ABSTRACT

Thermoplastic Olefins (TPO) possessing properties such as low density and recyclability are widely used in the automotive industry as a material of choice for numerous car parts and components. Scratch and mar damage reduces aesthetic value and is highly undesirable. Therefore, it is important to study the scratch and mar behavior of these materials. In this research TPO systems with and without scratch additive were injection molded at temperatures of 40°c, 50°c and 60°c be compared in terms scratch and mar behavior. All scratch and mar tests are administered on samples by a scratch machine using the ASTM standard D7027 method. Scratch behavior was studied using the onset of whitening as parameters judged by human observers and by the Automatic Scratch Visualization (ASV©) software. Visibility analysis of mar tests was done by checking for overall extent of visibility rather than simply the onset, and also by using contrast curves. Grazing incidence angle XRD was used to establish that surface crystallinity increases with mold temperature. Surface roughness results from the LSCM, scratch co-efficient of friction, and FTIR-ATR analysis were used to explain the behavior of scratch additive on the surface. Higher MFR systems show more dependence on mold temperature and show better scratch and mar behavior at higher temperatures. At higher mold temperatures, the scratch additive migrates better to the material, causing scratch and mar tips to slip and have lower co-efficient of friction and therefore, show delay in the onset of scratch and lower visibility for mar.

DEDICATION

I dedicate all the errors, flaws and poorly phrased parts of this thesis to myself, majorly imperfect as I am. I dedicate the good parts to you, little QT. I hope your tail's always wagging and your eyes, always shining.

ACKNOWLEDGEMENTS

I would like to thank my committee chair, Dr. H-J. Sue, for his advice, time, and for helping me evolve into a useful lab worker. Thanks to my committee members, Dr. Hong Liang, and Dr. Xiaofeng Qian, for their support throughout the course of my research. Their classes taught me a lot of relevant information and methods which helped me immensely, this work would not be possible without them. Surface Machine Systems made available the use of the scratch machine and the ASV© software, which enabled a major part of this research to be carried out.

Thanks also go to my colleagues and the department faculty and staff for tolerating me and teaching me, often repeatedly, the same procedures until I became fairly comfortable working by myself. Special thanks go to James, Shuang and Mohammad, the scratch team, who are the brothers I never had, each of them having their own amazing qualities which I look up to. I would also like to thank my department graduate advisor, Mrs. Philips Tandilyn for being ready to give me advice and imparting a sense of calm when I was in trouble.

Finally, thanks to my mother and father for everything.

NOMENCLATURE

TPO	Thermoplastic Olefin
XRD	X-Ray Diffraction
MFR	Melt Flow Rate
VLSCM	Violet Laser Scanning Confocal Microscope
SCOF	Scratch Co-efficient of Friction
ASV©	Automatic Scratch Visualization
PP	Polypropylene
JE1	Homopolymer PP, 4MFR
JE2	Homopolymer PP, 17MFR
JE3	TPO System without Scratch Additive
JE4	TPO System with Scratch Additive
DSLR	Digital Single Lens Reflex (camera)

TABLE OF CONTENTS

LIST OF FIGURES

Page

1. INTRODUCTION

In the words of Dr. H-J.Sue, it is nearly impossible to go an entire day without using or interacting with any polymeric material. Polymers are widely used in many industries for their easy availability, cheap cost, ease of processing and wide range of many physical and electrical properties which make them good fits for several applications. Even in the form of coatings, polymers are used on tools, consumer goods, industrial equipment, pipelines and in several other applications for enhancing surface hardness and resistance to friction [1]. The recent advancements made in the use of carbon nanotubes (CNT's) has also given rise to the possibility of introducing CNTs into polymer systems to enable modification of electrical and mechanical properties even further.

Polymers can be classified as thermoplastic and thermosetting polymers. Thermoplastic polymers exhibit softening on heating and can be molded into different desired shapes at high temperatures. They solidify on cooling and retain their shape but can be reshaped. Thermosetting polymers or thermosets are polymers which solidify permanently when heated. TPOs (thermoplastic olefins) are materials with low density High thermal stability and recyclability. These properties make them favorable for manufacturing several car parts and components. Since scratch and mar damage reduce the aesthetic appeal of these parts and also act as irregularities and stress concentration points for further damage on these parts, several efforts have been made to extensively study the scratch and mar behavior of polymers in the past. With the increasing use of

polymers in the electronics industry, especially on screens for cellphones and computers, there is a need to ensure that materials with best scratch resistance be used, or that the existing material's scratch resistance be improved by controlling processing conditions.

1.1: Previously used methods of scratch and mar behavior study

A scratch on a surface was defined as an asperity making a sliding indentation type of damage on a surface. Though this explanation serves to explain a part of the process to a layman, it does not cover many aspects of the scratch process. Especially in the case of polymers, where the viscoelasticity is a major factor contributing to the material's behavior, the testing and evaluation of scratch behavior requires more care in explaining the stress states experienced by the material during a scratch process [2]. Since polymers are materials whose behavior heavily depends on temperature and other working conditions, a testing method which yields reproducible results needs to be used while studying polymer scratch behavior [3]. In the past, there have been several methods proposed to study scratch behavior, both at the microscopic and macroscopic levels. At the macroscopic scale of testing, methods like the pencil hardness test require little equipment to carry out and there are other tests that require more sophisticated machines like the Taber test, pin-on-disc machine, single-pass pendulum sclerometer, Ford five-finger test and Revetest scratch tester. To perform scratch tests at smaller scales in microns or nanometers, there are many commercially available and customized test machines built by individual researchers. There are cases in which Scanning probe

microscopy instruments such as the Atomic Force Microscope have been modified to perform scratch tests at micro and nano-scales[4][5][6][7]. The use of Finite element studies and analysis is also very popular among researchers to emulate and explain the underlying mechanisms behind polymer scratch behavior [8]. The present-day Industry mostly uses the Erichsen method and the ASTM D7027 methods since these two methods are considered more quantitative compared to the previously developed methods. In the Erichsen method, a cross-hatched pattern is produced using dead loads and the difference in luminance of light scattered by the pattern and the luminance of light scattered by the background are considered as a quantity called "ΔL". In comparison, the ASTM method induces a single pass scratch by a tip which applies an increasing load at well-controlled conditions [9]

1.2: Scratch testing method ASTM D7027

The damage on the surface of materials has been classified as scratch and mar damage, scratch damage being caused by a single small tip at which load is concentrated. Scratches damage shows the formation of a groove due to material removal and mar damage is caused when another body slides on the surface and leaves a shallow but visible mark [10]. The ASTM D7027-13 standard describes a method of performing scratch and mar tests on a sample by using a scratch machine, shown in Figure 1, with an adjustable scratch tip and load range.

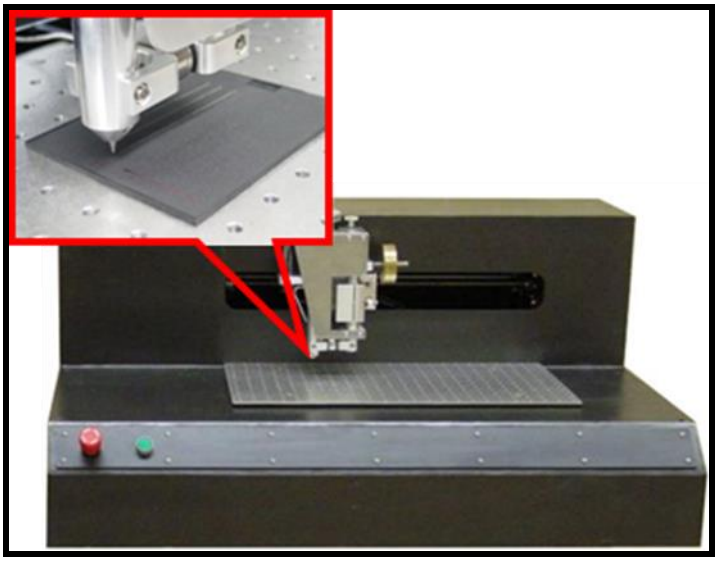

Figure 1: Scratch testing machine described by ASTM D7027

The sample being tested is clamped below the attached chosen tip and load range, test length and test rate are specified. A scratch or mar, depending on the tip used, is induced on the sample. A scratch process by this method can be broken down into three steps as shown in Figure 2, the Indentation step, during which the tip comes in contact with the surface of the sample, the scratch step, during which the tip passes over the surface while applying a load and causing deformation or damage, and a spring-back step in which the tip is withdrawn from the surface, marking the end of the scratch test [11] [12].

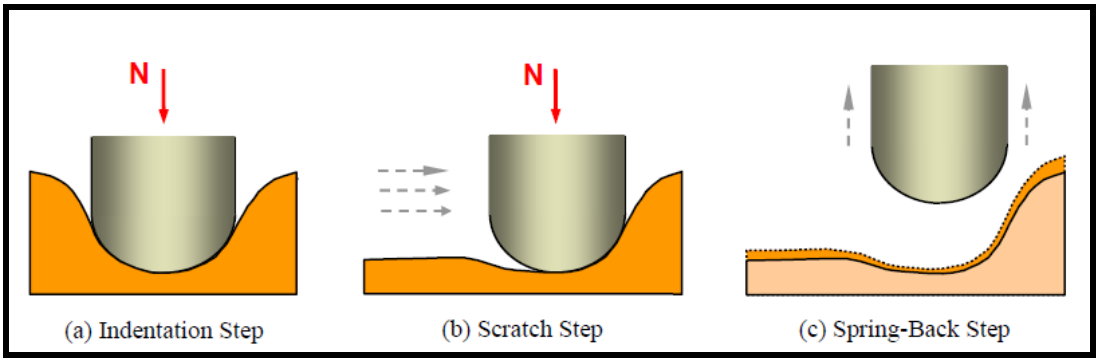

Figure 2: Steps of a scratch test [11]

Mar tests are different from scratch tests in that the depth of indentation is very negligible compared to a scratch test. The area of the tip is also usually much larger compared to the single-point contact of a scratch tip. Apart from these differences, the mar testing procedure is the same as scratch tests.

1.3: Damage to polymers due to scratch and mar tests

The work by H.Jiang et al categorizes polymers by their strength and ductility. Polymers with high modulus and ultimate tensile strength are classified as strong polymers, and those with high elongation before failure were classified to be ductile [11]. Scratch tests were conducted on four systems, polycarbonate (PC), Lexan 9034 which is a ductile and strong polymer, TPO with 70% polypropylene and 30% ethylene–propylene rubber, which is a ductile and weak system, polystyrene (PS), Styron 685D which is a brittle and weak system, and Epoxy, DER 332, which is a brittle and strong

system. Using the results of this work serves in explaining the different kinds of features observed when different types of polymers are scratched [11].

Under lower loads and stresses, the material undergoes a temporary deformation. This deformation is recoverable by the material and is barely visible if the material is allowed time for elastic recovery. For all types of polymeric material, brittle, ductile, strong or weak, this type of damage is common and was tentatively named “mar”, however, the term came to be later used for different type of damage altogether. The temporary deformation is caused by compressive stresses acting to indent the material and slide on it in the initial part of the scratch [11].

Figure 3 explains the fish-scale formation process. When the normal load applied increases beyond the point where the material can elastically recover, plastic deformation is observed in a repeating pattern called fish-scale or stick-slip pattern. When a very ductile material is subject to a scratch test, the scratch tip experiences two kinds of resistances to it progress in the direction of scratch. The first resistance is the kinetic friction between the scratch tip which is in contact with the surface of the material. The second resistance is due to the material build-up in front of the tip as it progresses in the direction of scratch. As the normal load increases, the tip penetrates deeper into the material and experiences more resistance ahead of it. When the magnitude of induces stress goes beyond the onset value for yielding, there is a fish-scale damage pattern formed through plastic drawing of the material. [11]

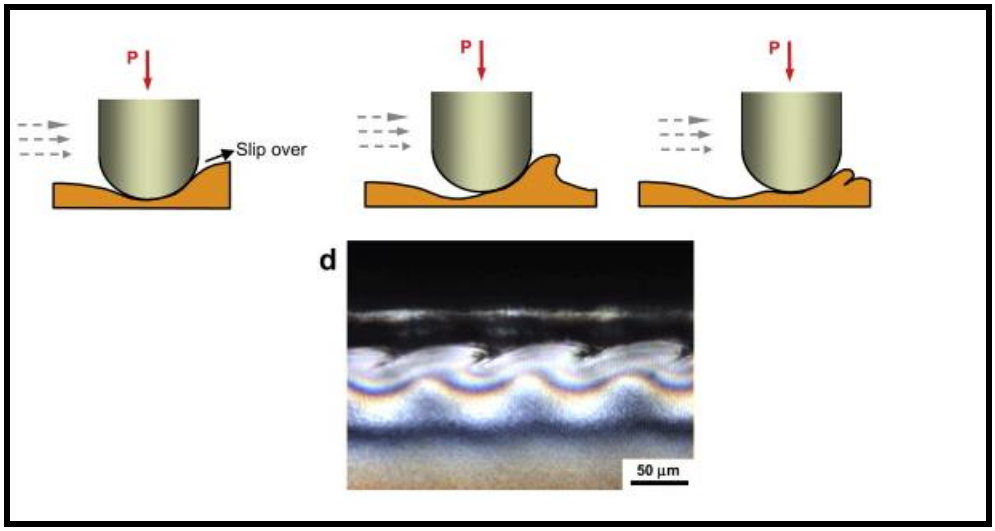

Figure 3: Formation of fish-scale feature [11]

When the load is high enough, there will be significant material removal from the surface. The tip penetrates into the material and the material built up in front of the tip will be “plowed” away to the sides of the tip to make way for the tip in the scratch direction. Plowing or material removal damage is the final stage of scratch damage.

Ductile materials show fish-scale and material removal zones and the onset load and severity depends on the yield strength and failure stresses of the material, but brittle materials often show other types of damage along with these usual fish-scale and material removal features. Crazing, voids, cracks and other kinds of damage features can be observed on scratches induced on brittle materials. Strain hardening features can also be observed in some polymers along their scratch directions. It is also often observed that brittle materials fail easily compared to ductile materials in nature, which holds in

the case of scratch damage too. Brittle polymers often show early onsets of different types of damage.

1.4: Quantifying scratch and mar visibility

Scratch damage on surfaces diminishes aesthetic appeal and also acts as a stress concentration site in case of parts built for withstanding loads. In case of metals, it can be much more catastrophic in the long run as scratch grooves and areas damaged by scratches act as origination sites for corrosion. This happens due to a difference in electronegativity created locally due to scratch damage. Polymeric coatings are a commonly used solution to avoid this type of damage [13], beside several other methods like sol-gel coatings [14], cathodic protection, sealants and anti-rust solutions [15][16][17]. But, since polymers are not as strong or hard as metals or ceramics in terms of modulus or ultimate strengths, they are more susceptible to scratch and mar damage, visibility study is a major concern for manufacturers since aesthetics is one of the primary issues and therefore it needs to be emphasized upon.

The human eye views objects and features on objects based on not the sole individual absolute brightness, but rather the Contrast of the object to its surroundings [18] [19] [20]. That goes without saying, a minimum intensity of light must be available for the eye to perceive an object, since no matter how colorful or highly contrasting the colors on an object, nothing is visible in a dark room without illumination. H.Jiang et.al

have quantified the contrast% to in the equation below, where C is the contrast and B_o and B_b are the brightness values of the object and background respectively.[18]

$$C = \frac{|Bo - Bb|}{B_o + Bb} \times 100\%$$

The color of an object also plays a role in the brightness of the object. Since all colors can be split into a combination of red, blue and green components, the brightness of an object in terms of the intensity levels of the individual red, green and blue components has been shown in the equation below, in which B is the brightness of the feature, R is the intensity of the Red component of light, G is the intensity of the green component and B is the intensity of the blue component contributing to the overall color of the object. [18]

$$\text{Brightness} = \mathbf{R} \times 0.299 + \mathbf{G} \times 0.587 + \mathbf{B} \times 0.114$$

In the case of both scratch and mar tests, contrast% is therefore used to quantify visibility rather than the individual brightness or intensity of light at the damaged region. The carbon black component in the samples serves to make the samples have the same color and therefore enables comparison between different samples.

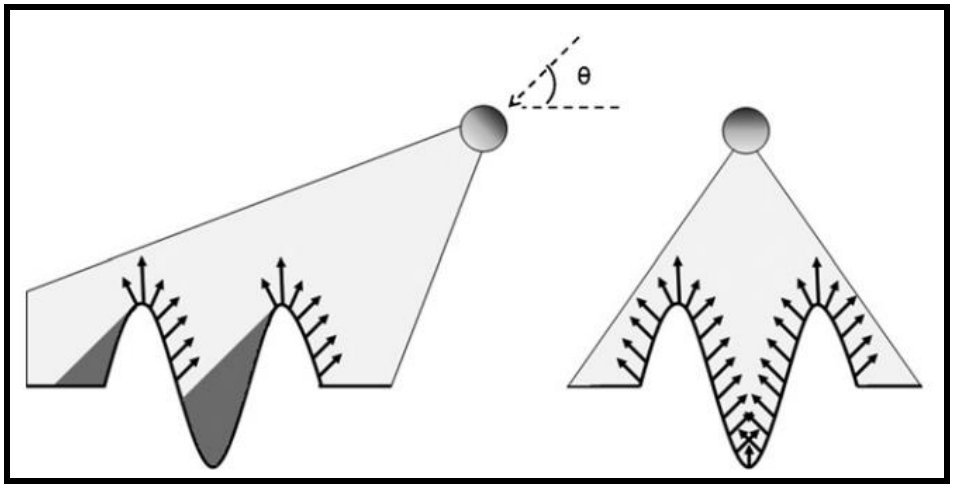

Figure 4: Illumination of a scratch path in various orientations [18]

Figure 4 shows a scratch path illuminated by a beam of light. When illuminated by an angular beam of incident light, scratch shoulders produce shadows and the trough or the scratch groove does not, giving an appearance of two lines with a different brightness in between them. Therefore, it becomes pointless finding the contrast% of a severe scratch. [18] It has been found in previous work that the onset of scratch coincides with a 3% contrast value. Therefore, the onset load of scratch is the parameter which is more important than the contrast at a heavily damaged area of scratch. In the case of mar, there is no severe sub-surface damage and the appearance is that of a gradually darkening or whitening scrape on a surface. Also, the 3% contrast value does not hold true for mar test onset of visibility. It makes more sense to quantify the mar with a contrast curve, rather than an onset value. Also, since mar damage is of two types, ironing (or smoothening), and roughening, there might be some interesting correlations between the surface roughness change along the length of mar to the visibility of mar in terms of contrast%.

1.5: Objectives

TPOs exhibit properties such as low density, high thermal stability and solvent resistance [21].They are also recyclable and have become increasingly used since the last few years in the automotive industry for manufacturing protective parts or decorative panels [22]. Damage due to scratches on the surface can be a precursor to failure by acting as regions of stress concentration and also reduce the aesthetic value of these parts. Therefore, Manufacturers aim to obtain surfaces with maximum scratch resistance [11]. This is often achieved by introducing additives like oleamides, erucamides and other fatty acids which serve in reducing friction improve scratch properties of materials. Injection molding is the most commonly used method in the production of polymeric parts, components and surfaces. The effect of processing conditions on the scratch and mar behavior of these polymers is focused on. In particular, the focus is on whether there are any chemical changes due to different processing conditions and whether or not there is a change in the scratch and mar visibility performance. The processing conditions in question are mold temperature, melt flow rates and the influence these conditions have on scratch additive performance. Whether or not there is a difference in behavior depends on the material properties which affect scratch and mar. Since a lot of related study has been done in the recent past, results from those studies and present experiments will be correlated to arrive at reasonable conclusions.

1.6: Previous results obtained using the ASTM D7027 standard

There have been several attempts at understanding scratch behavior of polymers using the ASTM D7027-05 method and finding out the dependence of scratch properties on other physical properties of the polymer such as young's modulus and yield strength. A few works which are relevant to the task at hand have been revisited in this section.

The relationship of material properties such as modulus, tensile strength, yield stress and co-efficient of friction to polymer scratch behavior was studied by C.Xiang et.al, using the Hamilton and Goodman scratch model which considers a scratch as an overlap between an indentation and a sliding process [24]. Although this work was done in 2001, there are several results which are relevant to the present study. A wide range of polymeric materials including PP and TPO systems were studied. Scratch tests were conducted on these materials at both constant and progressive loads. As shown in the Figure 5, the elastic modulus factors in at the indentation stage of the scratch process mostly, and affects the residual scratch depth after elastic recovery at indentation [24].

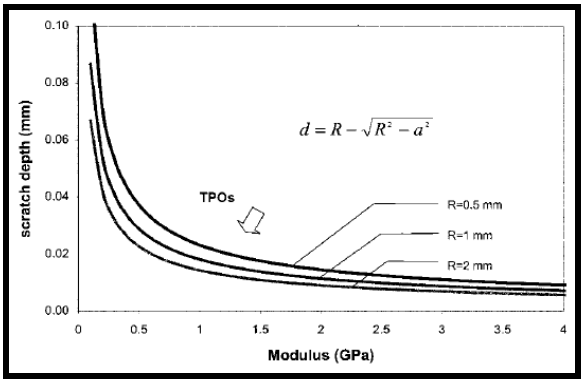

Figure 5: Relation between modulus and scratch depth [24]

It is shown that yield stress and tensile strength also dictate the type of damage and the extent of the plastic flow scratch pattern or the brittle fracture pattern. Polymers with higher yield stress values show smaller zones of plastic flow. If the tensile strength is lower than the yield stress, there is crack formation on the polymer surface. Since brittle damage is more easily visible than ductile damage, this scenario is better avoided. The effect of co-efficient of friction was also studied and it was found that there was presence of brittle damage such as cracking, crazing, de-bonding and cavitation wherever there were higher frictional values. Perhaps one of the most important conclusions from this work is the relationship between the modulus and the depth of scratch groove. Polymers with high moduli and show deeper scratch grooves, and therefore to resist scratch damage, polymers must possess a degree of rigidity [24].

A set of model TPO systems having different surface roughness values were tested by H.Jiang et al to study the effects of surface roughness and contact load on the scratch resistance of polymers [23]. The values of the samples and their surfaces are given in Figure 6.

Surface roughness values of model TPO systems

	Surface characteristic	R_a (μm)
Sample #1	As-received surface	0.5 ± 0.02
Sample #2	Wet-grinded	1.7 ± 0.07
Sample #3	Wet-grinded	2.5 ± 0.11
Sample #4	Wet-grinded	4.5 ± 0.21
Sample #5	As-received "Animal Skin" texture	17.8 ± 0.92

Figure 6: Sample surface roughness values of TPO systems [23]

Scratch test conditions for this study were carried out in compliance with the method described by the ASTM D7027 standard. The scratch tip used for the tests was a commercially obtained stainless steel Grade 25 bearing ball with a diameter of 1 mm, with a maximum roughness value close to 50 nm. Other important criteria are a scratching speed of 100 mm/s, a normal load range of 1–40 N, and a 100mm scratch length. Digital load cells equipped on the scratch machine recorded the normal and tangential loads experienced by the tip on the surface. [23]

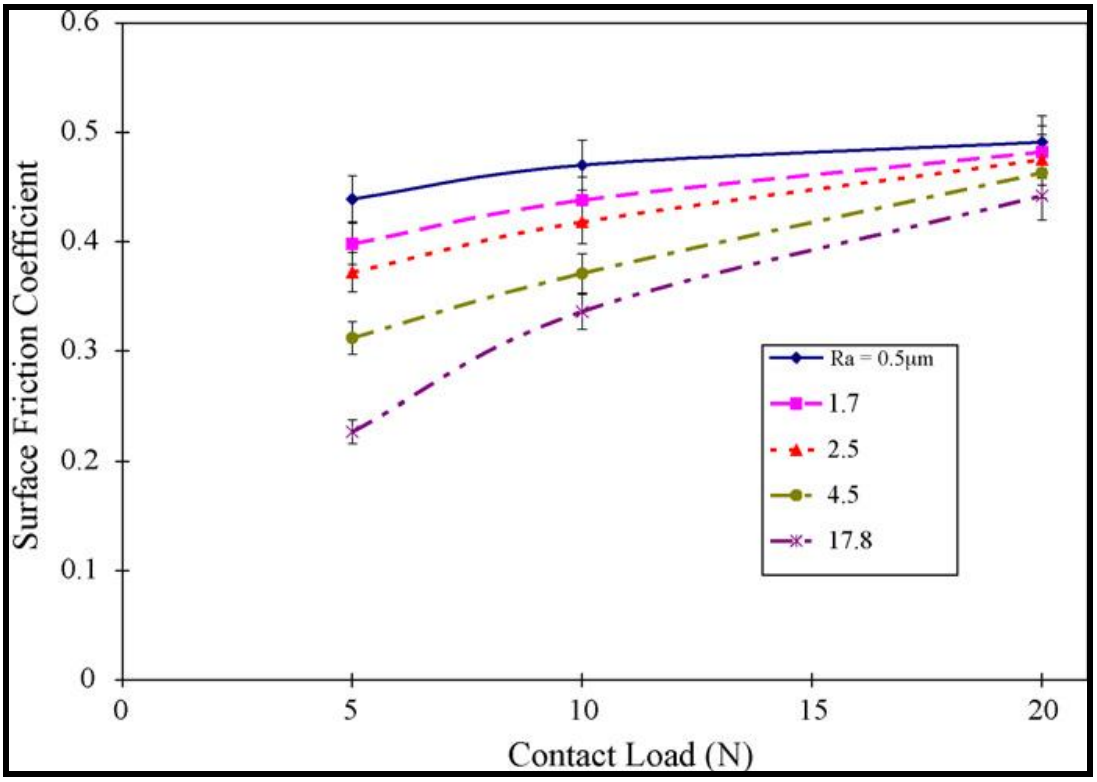

Figure 7: Relation between surface roughness, contact load and SCOF [23]

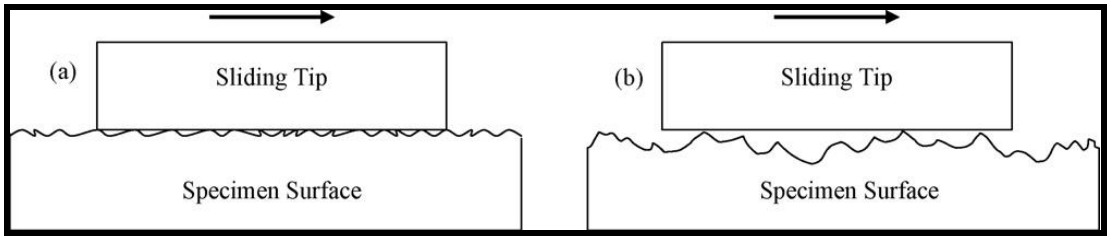

Figure 8: Representation of a tip sliding on surfaces of different roughness [23]

The results from these tests, shown in Figure 7, gave the conclusion that since there will only be contact at a few points on the surface, not all, and the number of points or the area of contact depends on the surface features of both tip and surface. As shown in Figure 8, Even if a surface is rough, it will have few contact points if the scratch tip is very smooth and therefore, a smaller area of contact would be experienced by the tip and surface. The tangential force of resistance is lower if there is a lower area of contact. Since the co-efficient of friction directly depends on the resisting tangential force, the value of co-efficient of friction is also lowered. When a higher load is applied during the scratch process, the scratch tip will locally compress the asperities on the surface of the sample. This will cause an increase in the area of contact between the tip and surface, and will be reflected as a higher co-efficient of friction. Also, another part of this study focuses on the effect of the presence of surface-treated erucamide additive. It is found that this additive causes most effect in the SCOF for the lower loads of scratch, and surface treatment is done to cause migration of the slip agent to the surface, which improves frictional properties and therefore lowers scratch damage and visibility.

Work done by Browning et.al is very closely related to the task at hand, in terms of addressing the effect of molecular weight on scratch behavior. They were able to

associate the onset of fish-scale formation to the ultimate tensile strength of the material, and also compared the scratch test results of different molecular weight systems [25]. The conclusion from that study was that increasing the molecular weight improves the tensile strength and ductility of the material. Since the formation of periodic stick-slip or fish scale pattern on a scratch depends on the tensile strength, the onset of fish scale was delayed as the molecular weight of the samples used was increased. In the present study, there is an effort made to learn the effect of melt flow rate on scratch behavior. Since melt flow rate and molecular weight are factors that can be inversely related, the results obtained can be correlated to the results obtained by browning et al, and scratch and mar phenomena can be explained more convincingly.

1.7: Model systems and experimental conditions

Sample System	Polymer
JE1	4 MFR Homopolymer PP
JE2	17 MFR Homopolymer PP
JE3	20% Talc filled TPO without scratch Additive
JE4	20% Talc filled TPO with scratch Additive

Figure 9: Sample systems, material and processing conditions

Figure 9 shows the four model systems used. The systems JE1 and JE2 are homopolymer PP plaques of dimensions 150mm x 100mm x 3mm, molded at different

melt flow rates of 4 and 17 respectively. Systems JE3 and JE4 are TPO plaques of the same physical dimensions, the difference between them being that a scratch additive is present in the polymer matrix of JE4, absent in JE3. All systems contain 1% carbon black pigment which is to enhance visibility of scratch and mar induced on them. Each model system has plaques molded at temperatures of 40˚c, 50˚c and 60˚c.

Surface Roughness(Rq)	40^0c	50^0c	60^0c
JE1	2.965±0.11	2.81±0.19	3.041±0.086
JE2	3.005±0.04	3.13±0.12	3.011±0.039
JE3	2.12±0.065	2.203±0.015	2.33±0.061
JE4	2.06±0.069	2.222±0.255	2.231±0.078

Figure 10: Virgin surface roughness (Rq) of sample systems

Before conducting any scratch or mar tests on the samples, the surface roughness of the undamaged virgin area was calculated by using VLSCM, shown in Figure 10, using a magnification of 10x, for an area of 1350um x 1012um. The surface roughness values in figure 2 indicate that there is no predictable pattern to surface roughness of samples with mold temperature.

The scratch additive's effect on virgin area surface roughness shows no pattern. JE3 samples do not consistently show higher or lower virgin surface roughness compared to JE4 samples. But, with increasing mold temperature, there is an increase observed in the surface roughness of the JE3 and JE4 systems.

2. GRAZING INCIDENCE ANGLE XRD

The MFR used during the injection molding process has a direct effect on the molecular weight of the resulting polymeric chains, as described in previous sections. Crystalline regions on a polymeric surface are simply areas where polymeric chains have untangled and aligned themselves in a somewhat ordered fashion. To understand the trend of surface crystallinity of the polymers, grazing incidence angle XRD is carried out on all samples at an incidence angle of 0.5°. The equipment used is the Bruker D8 Discover in detector scan mode with data being obtained at every 0.07° interval. The XRD peaks and data obtain correspond to a maximum of 100nm of the surface of the samples, since the angle of incidence used is so low. The XRD peaks obtained for the four systems molded at 50°c are shown below in Figures 11, 12, 13 and 14 as a representation;

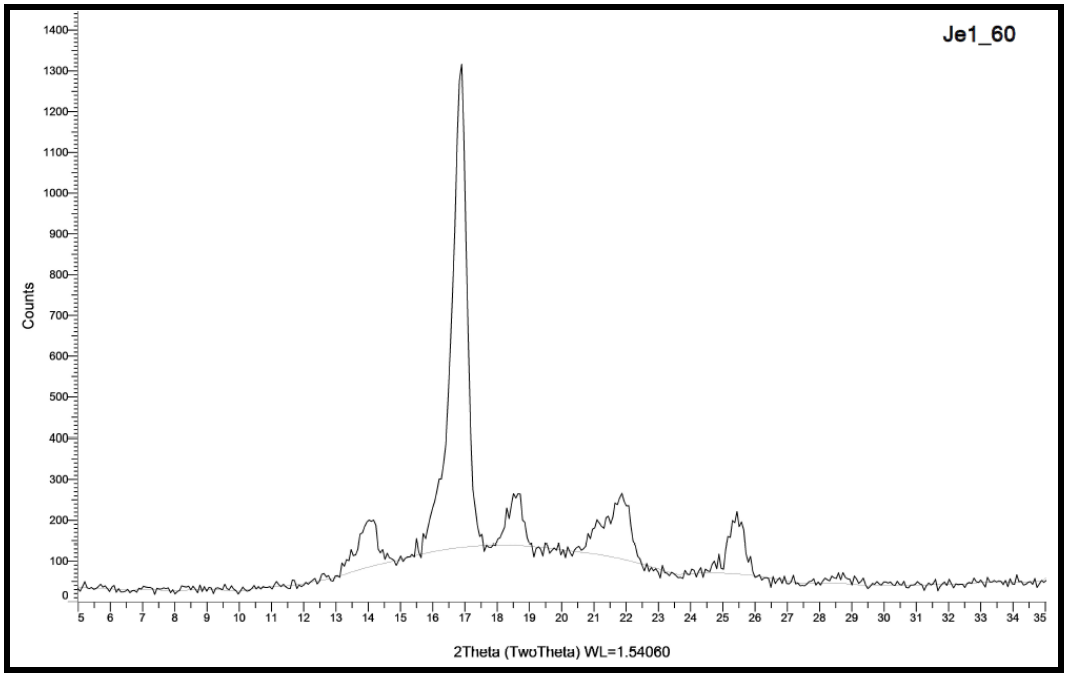

Figure 11: XRD peaks of sample JE1_60

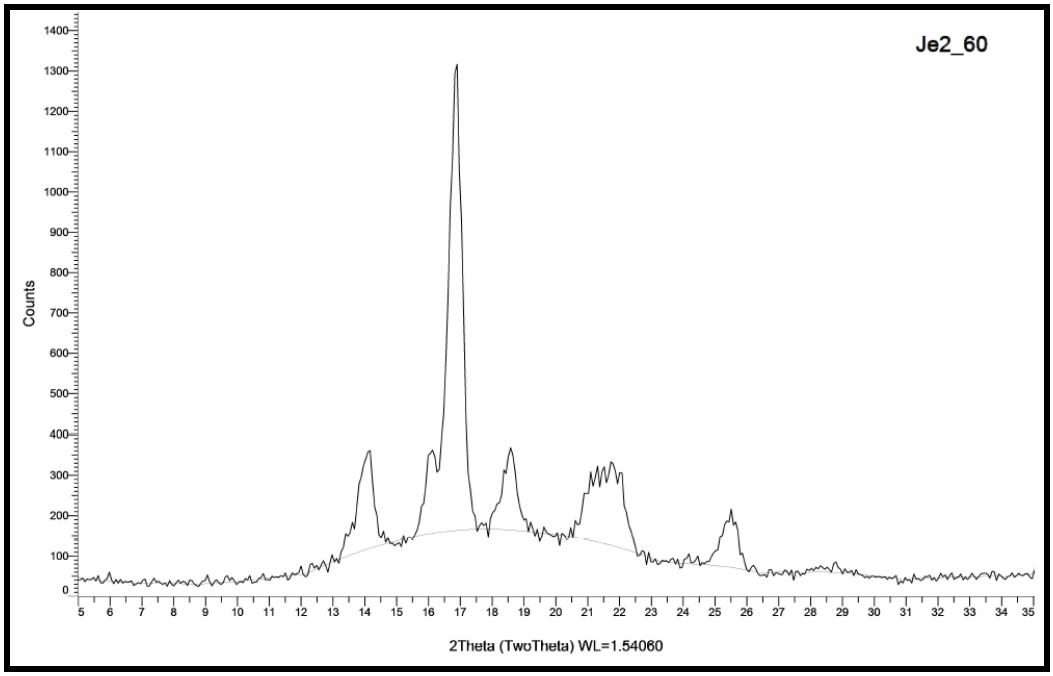

Figure 12: XRD peaks of sample JE2_60

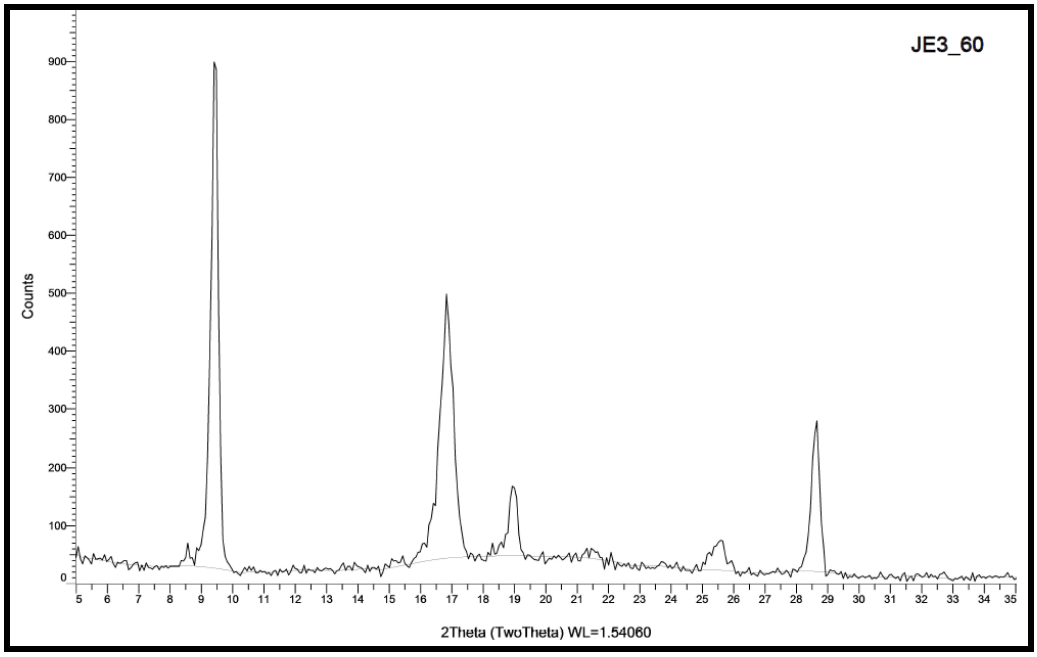

Figure 13: XRD peaks of sample JE3_60

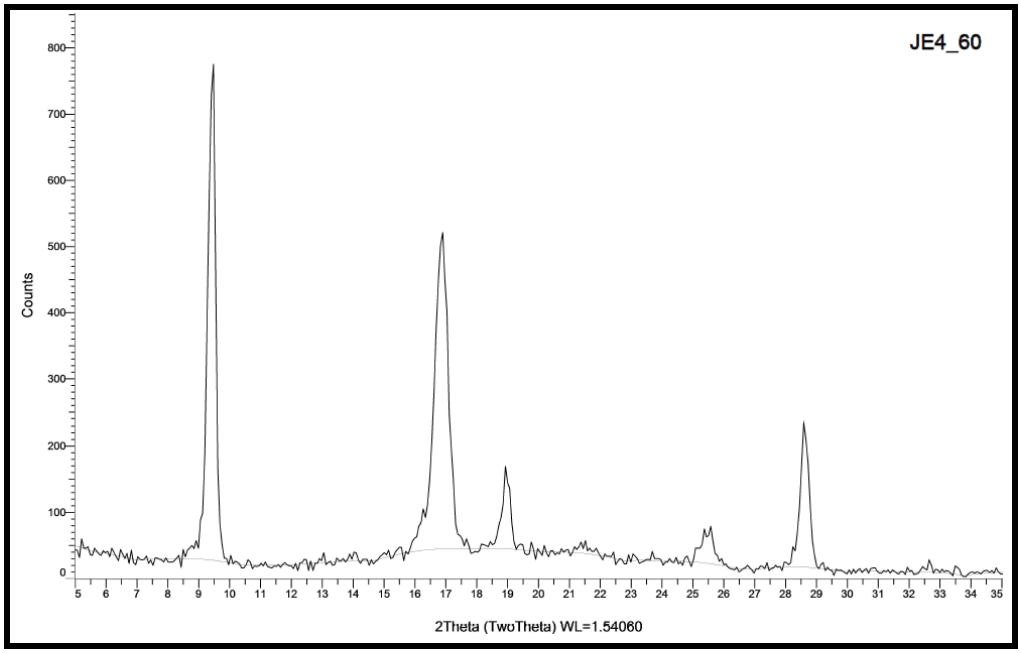

Figure 14: XRD peaks of sample JE4_60

Resulting Grazing angle-XRD peaks were analyzed for percentage crystallinity using the formula:

$$\% \text{ Crystallinity} = \frac{\text{Area of crystalline region}}{\text{Area of amorphous region+Area of crystalline region}} \text{ x } 100\%$$

The surface crystallinity of the sample systems is shown in Figure 15:

Crystallinity%	40^0c	50^0c	60^0c
JE1	47.1	55.85	49.89
JE2	51.01	52.22	54.34
JE3	46.8	50.3	52.1
JE4	42.4	48.33	51.4

Figure 15: Surface crystallinity of model systems

Crystalline regions in a polymer are regions where the polyeric chain molecules are better aligned compared to the bulk material. These regions are formed at the expense of heat energy available at the surface of the material. Therefore, it can be understood that polymers molded at higher tempratures would exhibity higher surface crystalinity.

At low MFR, as explained in the previous sections, polymeric chains have higher molecular weights. This indicates that the molecules would be longer and subsequently, more entangled and more randomly aligned to begin with. The effect of mold temperature is therefore countered due to the increased randomness and intertwining of the molecules in the system, and the system JE1 does not show the normal trend of increasing surface crystallinity with mold temperature.The effects of surface crystallinity on the polymer scratch and mar behavior will be studied and addressed in the following

sections, along with the effect of surface crystallinity compounded with the effect of scratch additive on the system.

3. FTIR-ATR ANALYSIS

The purpose of the FTIR-ATR analysis is to check whether or not there is a chemical change in the samples due to variation in manufacturing or processing conditions. The presence of a tangible difference in the FTIR spectra, appearance of a new peak or a missing peak, would indicate the presence or removal of a certain chemical bond and therefore a component from the system. FTIR-ATR analysis was carried out using a Nicolet 3800 FTIR machine at absorbance format. All samples were tested at settings of 50 scans, 4 resolution and at absorbance format with atmospheric suppression.

3.1: Effect of melt flow rate and mold temperature

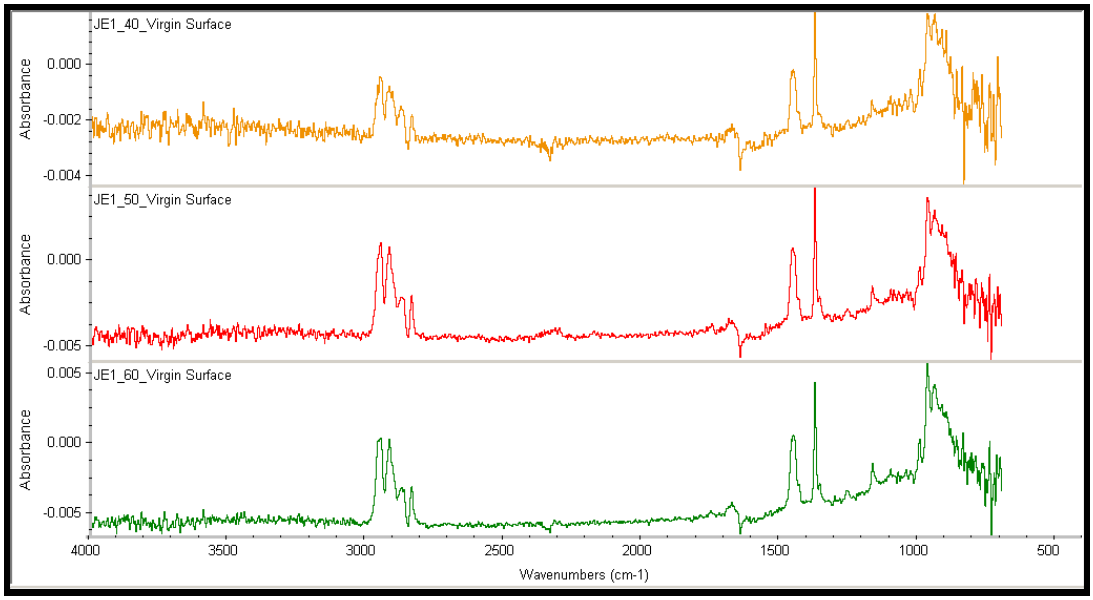

Figure 16 : FTIR spectra of system JE1

As shown in Figure 16, in system JE1, at low MFR, there is no difference in the FTIR graphs. The peaks between 2800-3000 cm^{-1} correspond to stiff sp3 C-H bonds, [26] [27] [28]. The peaks at around 1300 cm^{-1} can be linked to aromatic CH and carboxyl-carbonate structures [29] [30] [28]. The peak at 2350 cm^{-1} corresponds to residual CO_2 [31] [32]. Overall, there is no significant difference between the FTIR-ATR Spectra of samples at all the different temperatures, and it can be stated that changing the mold temperature does not alter the chemical composition of the material in any way.

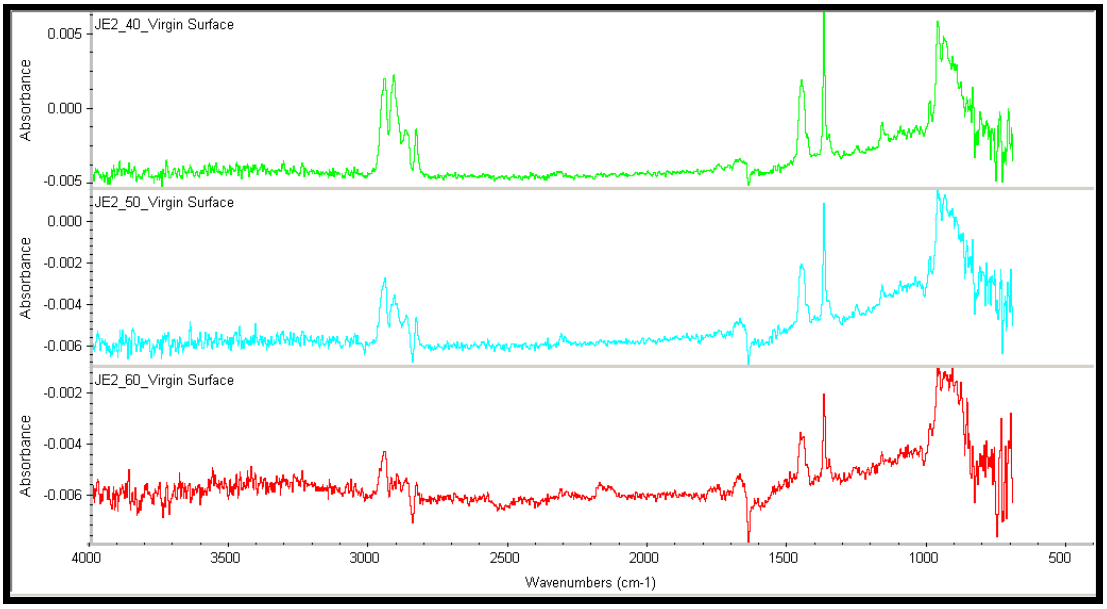

Figure 17: FTIR spectra of system JE2

In Figure 17, The FTIR spectra of the sample system JE2 of 17MFR show more variation in height of peaks compared to the 4MFR system. The points of interest are the peaks at 2800-3000cm^{-1}, which correspond to stiff C-H bonds and the peaks at 1650-

1700cm^{-1}, which correspond to C=O bonds[33][34]. As mold Temperature increases, the peaks at 2800-3000cm^{-1} become less and less prominent and the peaks at 1650cm^{-1} become sharper. This suggests that there are no new chemical bonds associated to higher mold temperature, but there is a decrease in the number of stiff C-H bonds on the surface of the material and increase in the C=O bonds.

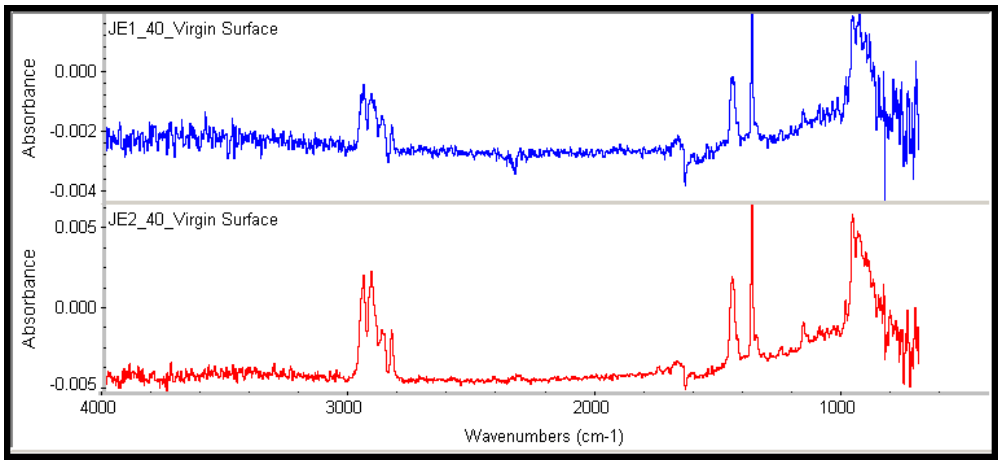

Figure 18: FTIR spectra of JE1 vs JE2, 40 degrees Celsius

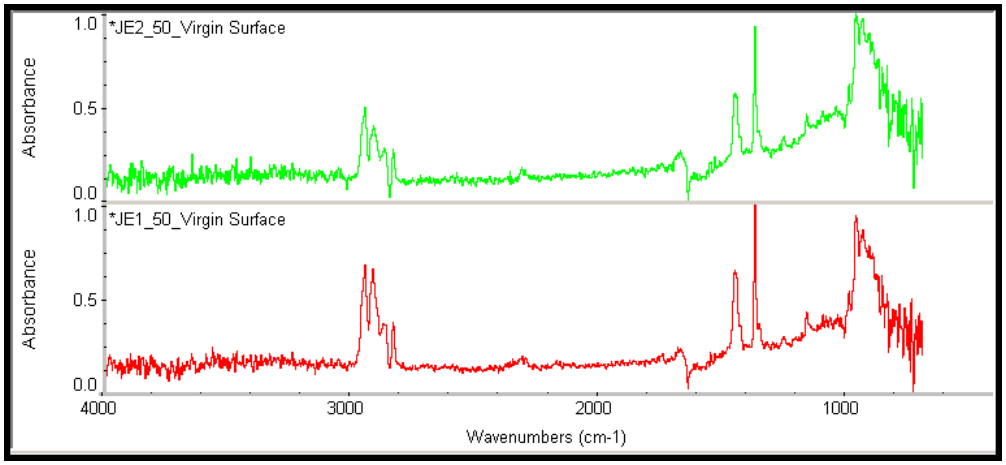

Figure 19: FTIR spectra of JE1 vs JE2, 50 degrees Celsius

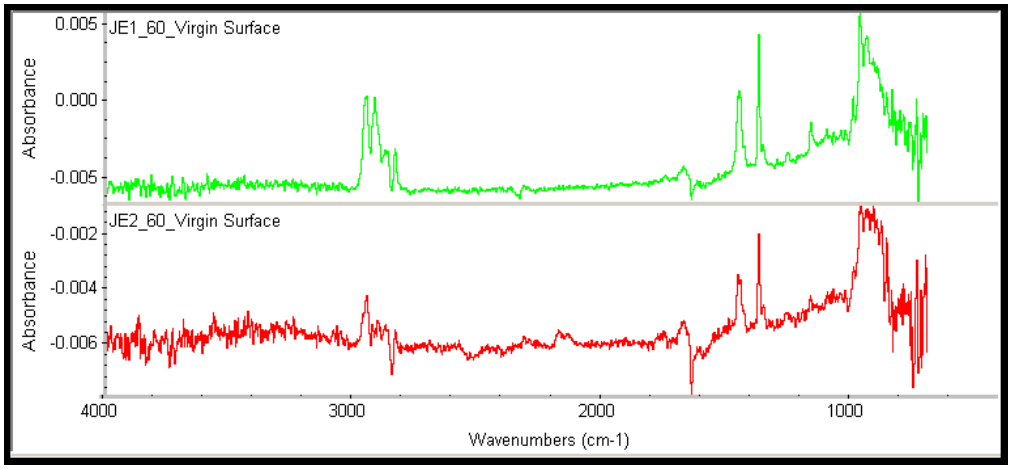

Figure 20: FTIR spectra of JE1 vs JE2, 60 degrees Celsius

Figures 18, 19 and 20 compare both JE1 and JE2 system FTIR spectra. Between JE1 and JE2, there is no major difference in the spectra of the two systems, except that the JE2 system, which has higher MFR, is more variant with mold temperature than the low MFR system. Both systems tend to exhibit a residual CO2 peak at 2350cm^{-1}, especially at higher mold temperatures.

3.2: Effect of mold temperature on additive behavior

The FTIR-ATR spectrum of the JE4 system is similar to the JE3 system, as shown in Figures 21 and 22, with the exception of peaks at 1650cm^{-1}, and 3300-3400cm^{-1}. These two peaks correspond to the amide group and symmetric and asymmetric stretch absorptions of primary and secondary amines respectively [35] [36]. Since these peaks

are not very prominent in the JE3 system, they are the difference between the two systems, i.e., they correspond to the slip agent used.

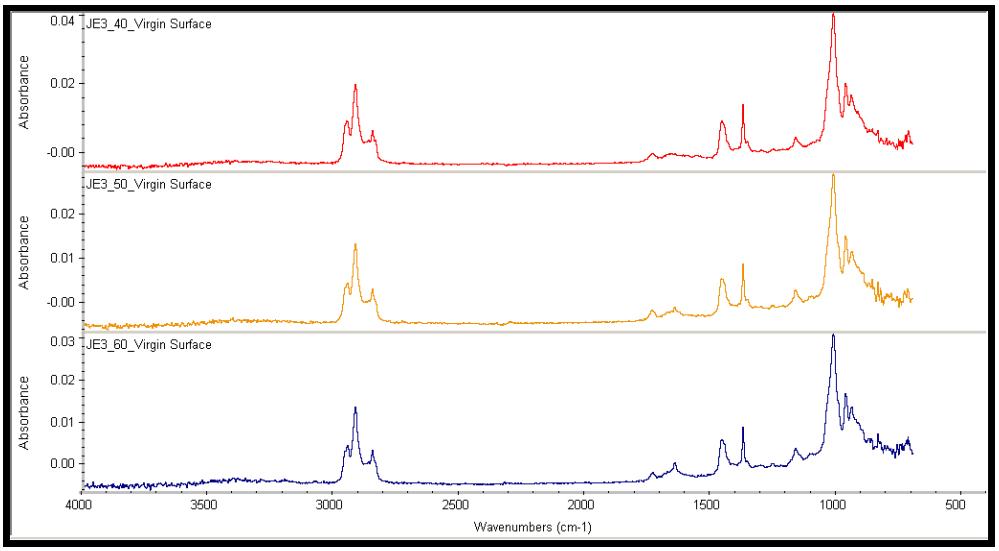

Figure 21: FTIR spectra of system JE3

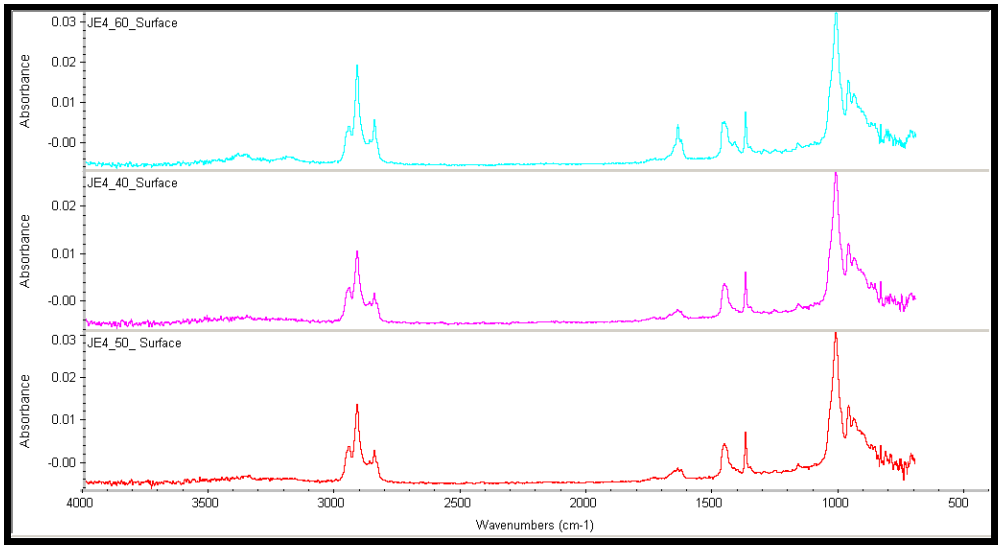

Figure 22: FTIR spectra of system JE4

The peak at 1650cm^{-1}, which corresponds to the amide group, increases in sharpness with increasing mold temperature. A similar trend is followed by the peaks between 3300-3400m^{-1} as well, although at a lower scale. Increasing the mold temperature permits more energy in the system and allows for the polymeric chain molecules to have a higher freedom of motion. In turn, this allows migration of the scratch additive to the surface more freely. Since the FTIR analysis was done on the surface of the samples, it can be concluded that the presence of the slip agent on the surface is more prominent for samples molded at higher temperature. This could be a useful tool in explaining differences in mar behavior. Since scratch damage happens below the surface, running an FTIR analysis below the surface of the sample at a depth of 200um was considered for system JE4.

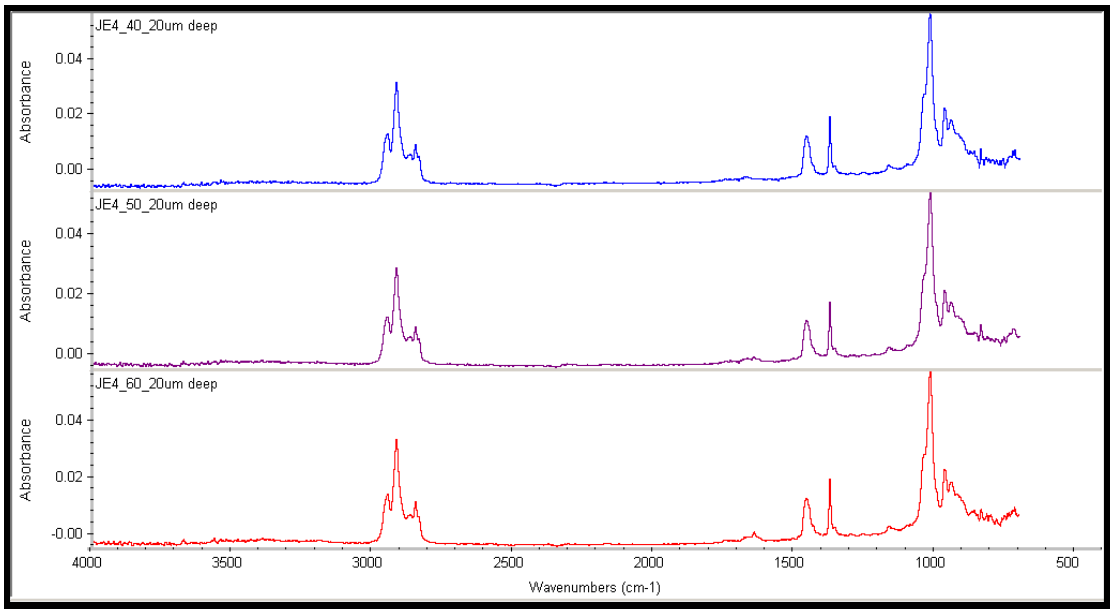

Figure 23: FTIR spectra of 200um depth below the surface of system JE4

The top 200um of the surface of the JE4 samples was polished using a polishing machine with 1200grit sandpaper as the abrasive, and then the sample was dried and cleaned with a blast of high purity nitrogen gas. FTIR analysis was carried out on these surfaces and the result obtained, shown in Figure 23, shows small, very vague peaks at the wave numbers corresponding to the scratch additive. From this, it can be said that the presence of the scratch additive is in less than the top 200um of the surface, and that higher mold temperature allows free migration of scratch additive to the surface and this in turn could impact scratch and mar behavior, especially the friction component.

4. SCRATCH TESTS

4.1: Scratch testing criteria

Figure 24 : 1mm diameter stainless steel scratch tip

Scratch tests were carried out using a 1mm diameter steel ball scratch tip as shown in Figure 24. The load range used for all tests is a progressively increasing load of 1-50N over a scratch length of 100mm, (1N at the start of the test at 0mm to 50N at 100mm). Tests are carried out at three different rates of 1mm/s, 10mm/s and 100mm/s. All analysis is done on both scratch and mar tests after allowing at least 48 hours of time for elastic recovery of the material. The onset of different types of damage, fish scale and material removal, are the parameters to compare the scratch behavior, also, since aesthetics is a primary concern in scratch, the onset of whitening is used to compare the scratch behavior of these materials. To find the onset points of whitening, the plaques are scanned using an optical scanner and analyzed by the ASV© software with 3%

contrast and 50% continuity. These values are selected since they have previously been reported to closely match human observation. Human observers were also asked to judge the onset of whitening under a controlled lighting condition, the sample being placed in a black box in a dark room, illuminated by a single light source. Observers' reading of the onset of scratch visibility and whitening was also noted to be compared to the ASV results to get an even more accurate estimate of the onset points.

4.2: Onset of visibility study

For both scratch and mar tests, Analysis was done by using the ASV© software and also by three human observers whose readings were kept unknown to one another, to avoid any influence on each other's views. In the past, it has already been shown that the ASV© software gives results in tune with human visibility [9] [18]. To begin to analyze and explain further phenomena, it was first necessary to compare human observer's readings to the ASV readings so that one of the two sets of data could be chosen for further discussion on topics.

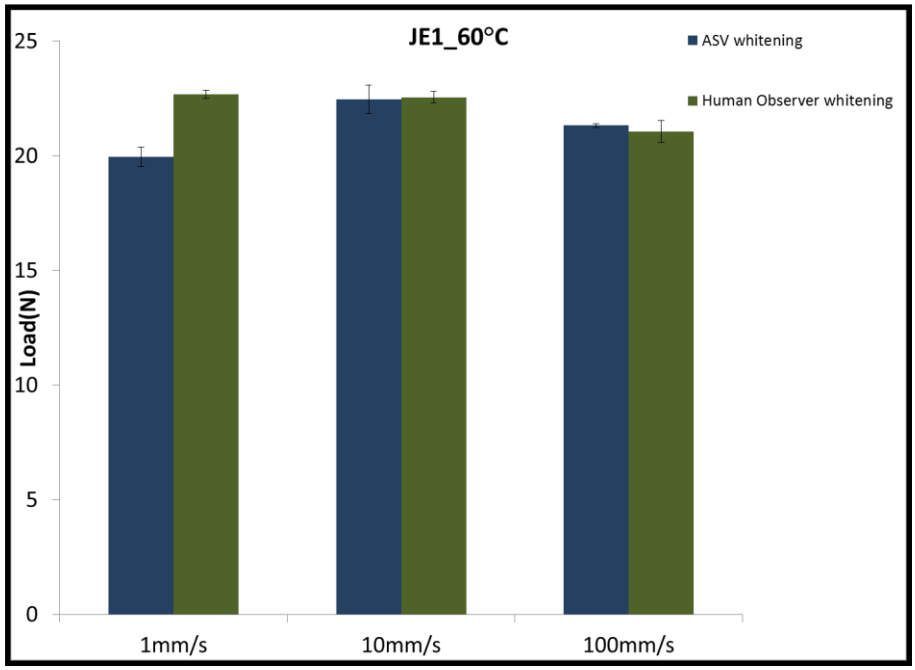

Figure 25: Onset of visibility, JE1_60

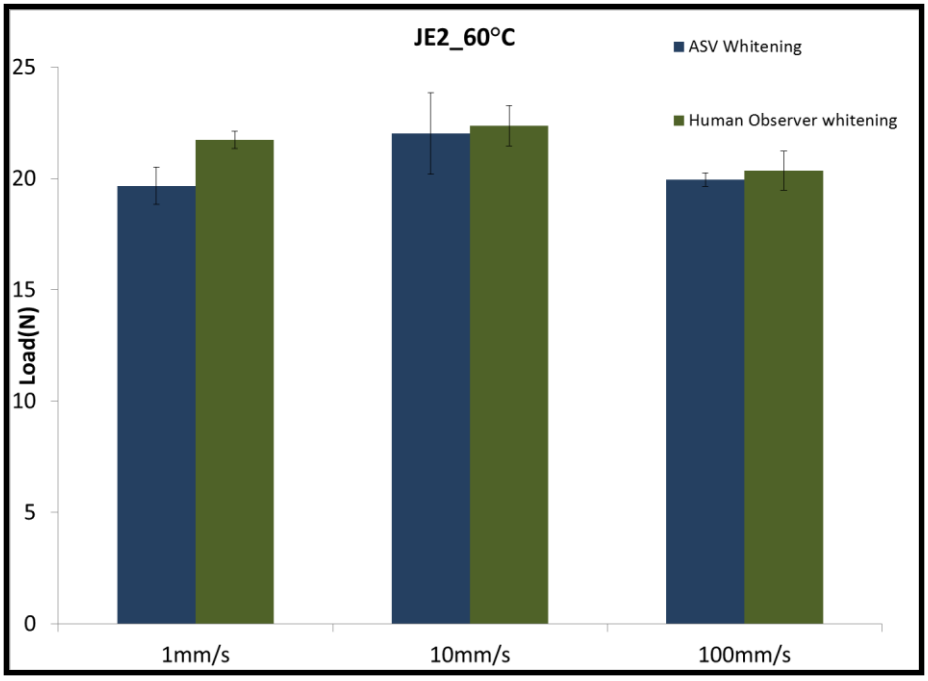

Figure 26: Onset of visibility, JE2_60

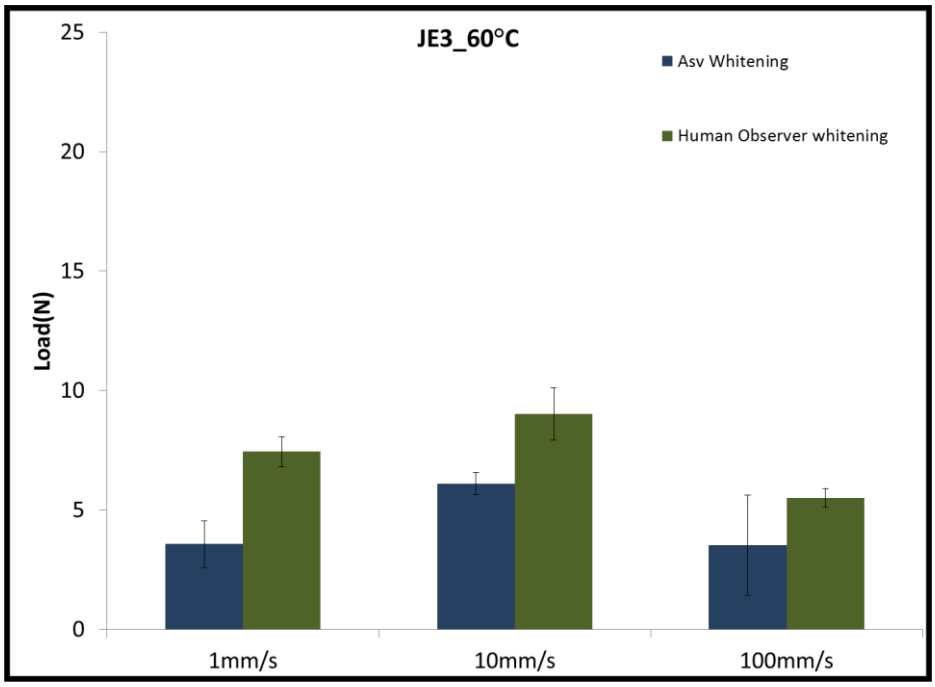

Figure 27: Onset of visibility, JE3_60

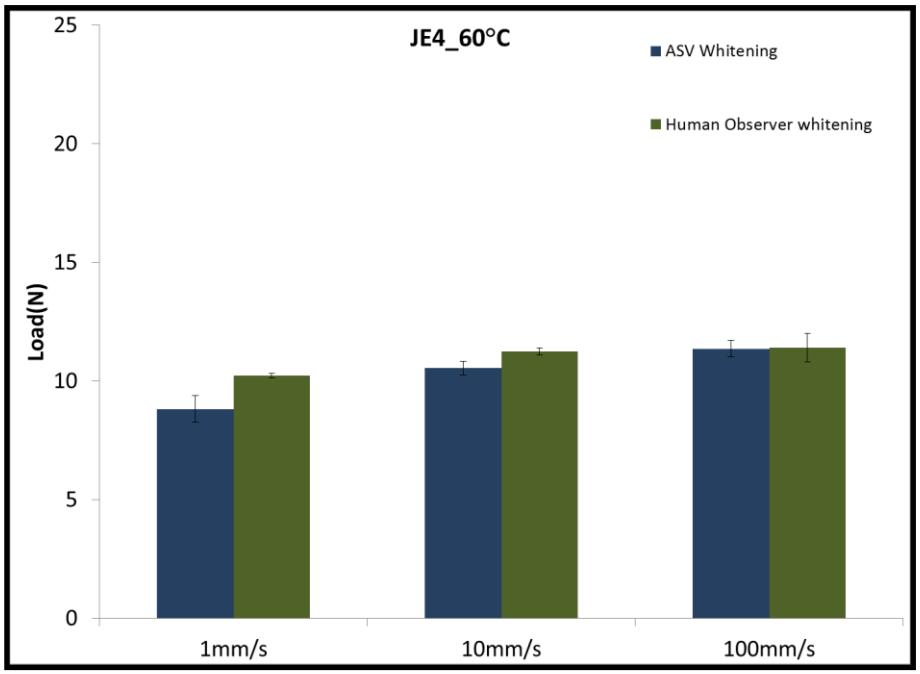

Figure 28: Onset of visibility, JE4_60

The Figures 25, 26, 27 and 28 are comparisons between the human observers' perception of the onset of visibility and the ASV software results. To obtain the onset of visibility, since the initial damage is darkening damage, the criteria input to the ASV was +3% contrast and 50% continuity.

Human observers and ASV results for whitening are comparable and show very close values in all samples. In a few cases, the ASV shows slightly delayed onset of visibility of scratch compared to human observers. This difference of approximately 2N can be attributed to the human observers having the freedom to adjust their stance or adjust their position, neck tilt, or viewing angle slightly to improve clarity of vision. The onset of whitening data is interchangeable for both human and ASV results, Human observation is taken as the preferable data set while addressing future comparisons and analysis in the research.

Scratch resistance of a sample can be quantified by the onset of damage and visibility of the sample. A material with better scratch resistance will show a delayed onset of damage and a delayed onset of visibility. The onset of damage and visibility for each scratch are found using the ASV© software and also human observation by three independent observers whose readings were not revealed so as to avoid any prejudice while conducting the experiment.

The figures 29, 30 and 31 are graphs showing the onset of whitening of sample systems.

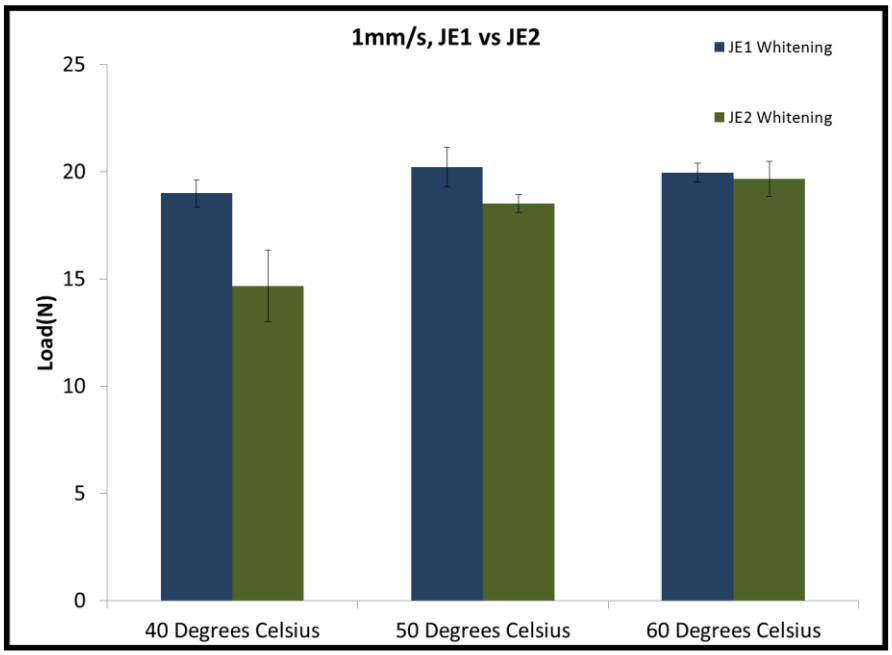

Figure 29: Onset of visibility, 1mm/s, JE1 vs JE2

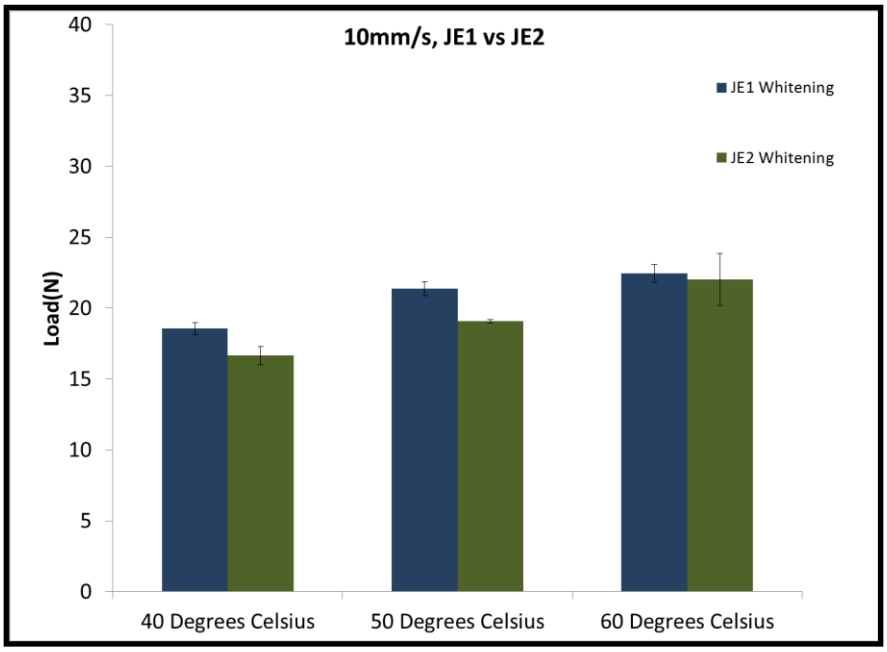

Figure 30: Onset of visibility, 10mm/s, JE1 vs JE2

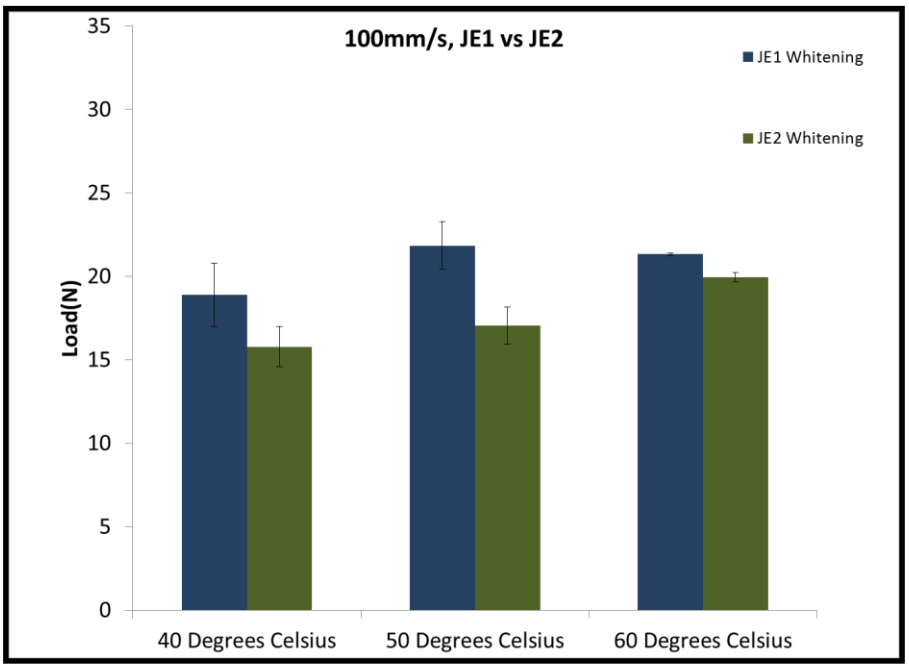

Figure 31: Onset of visibility, 100mm/s, JE1 vs JE2

The Onset of whitening of the JE1 system (4MFR) is delayed compared to the JE2 system (17MFR) for all scratch tests. The MFR of a polymer can be correlated to the molecular weight by an inverse relation [37]. Previous work by Browning et.al suggests that increasing the molecular weight would increase the tensile strength of a polymeric system, which can be used to explain the obtained result.

At 4MFR, System JE1 shows no clear trend in the onset of whitening varying with mold temperature at any rate of testing. For any mold temperature, the onset of visibility of scratch is almost the same. However, at a higher MFR of 17, System JE2 shows a clear trend of the onset of whitening being delayed with increase in the mold temperature. Increasing the MFR makes the sample's Onset of whitening more sensitive

to mold temperature and a higher mold temperature accompanied by a higher melt flow rate shows the most delayed onset of whitening at all rates.

From the results of previous work as discussed, molecular weight and MFR are inversely related. The lower MFR system corresponds to a higher molecular weight. It has been shown that increasing the molecular weight of a system increases the modulus and strength and therefore delays scratch visibility. Also, the low MFR means that chain molecules are longer, more entangled, and have less freedom to orient themselves. This translates to the surface crystallinity% of the system. The system with higher MFR shows increasing trend of crystallinity with mold temperature, and follows no such trend for the system with low MFR. Therefore, the mold temperature must have lesser effect on the lower MFR system compared to the higher MFR system, which is also observed in the graphs. Results shown in figures 32, 33 and 34 are used to study the effect of scratch additive and mold temperature on the onset of visibility and whitening.

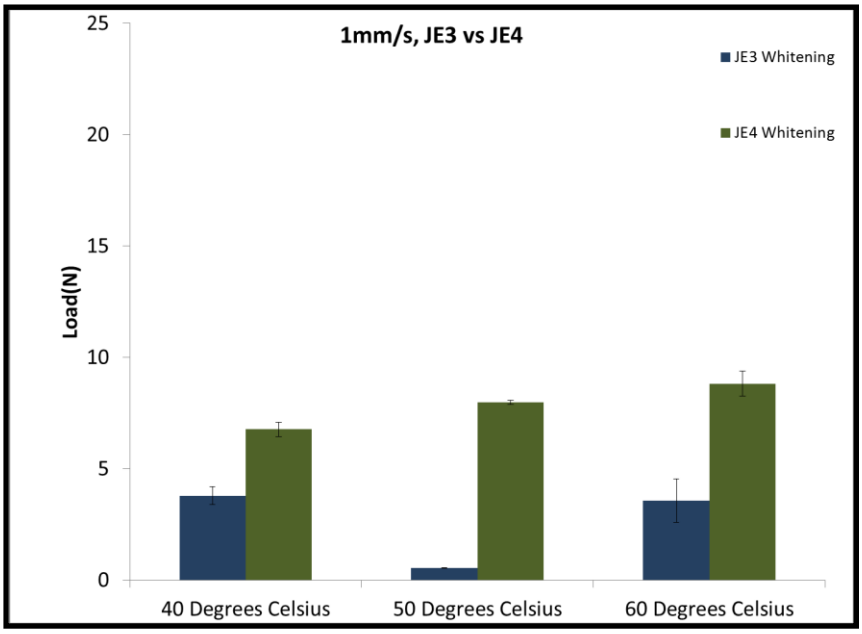

Figure 32: Onset of visibility, 1mm/s, JE3 vs JE4

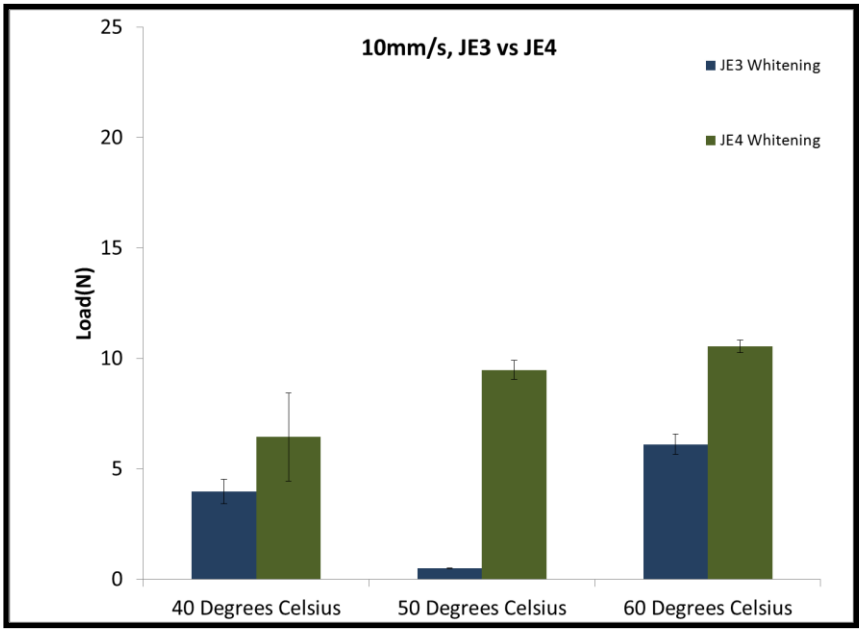

Figure 33: Onset of visibility, 10mm/s, JE3 vs JE4

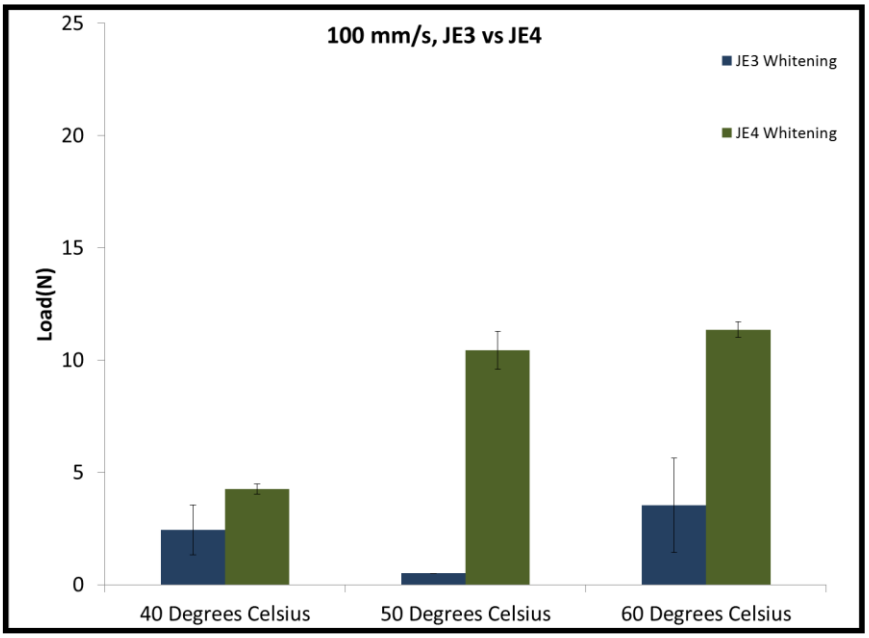

Figure 34: Onset of visibility, 100mm/s, JE3 vs JE4

The scratch behavior of System JE3 shows much earlier onset of visibility than system JE4, as expected. As the mold temperature increases, the onset of visibility of scratch on the JE4 system increases. Since the system without additive does not show any particular trend in scratch behavior with mold temperature, it can be assumed that the difference in the onset of visibility of scratch of the JE4 system is not due to the change in behavior of the material, but due to the change in behavior of the additive in the material at higher mold temperatures.

This can be related to the fact that the scratch additive shows better migration to the surface of the material, as was found in the FTIR-ATR analysis results for systems JE3 and JE4. The surface crystallinity of the systems increases with mold temperature for both these systems. But, by observing that system JE3 does not exhibit delayed

visibility with mold temperature, it can be concluded that the effect of additive is much more relevant and important regarding scratch visibility than the surface crystallinity.

4.3: Onset of fish scale and plowing damage

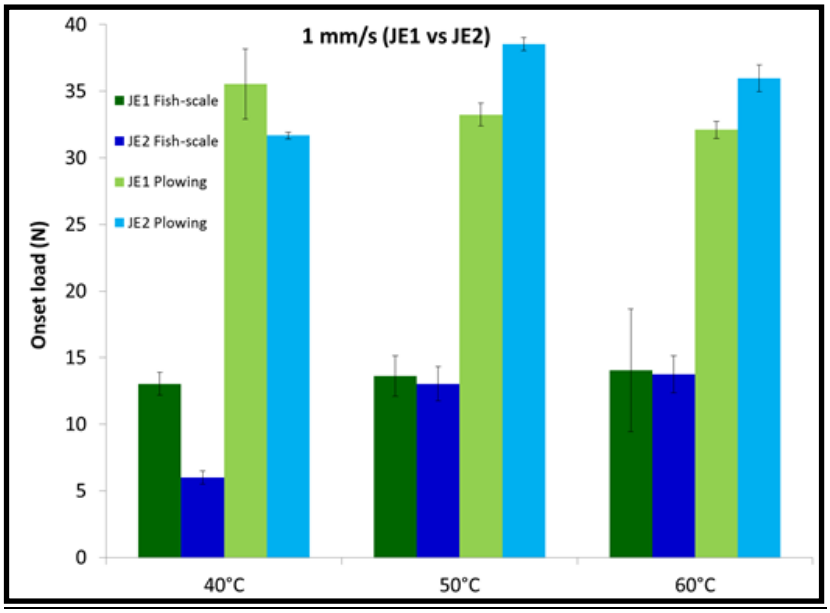

Figure 35: Onset of damage, 1mm/s, JE1 vs JE2

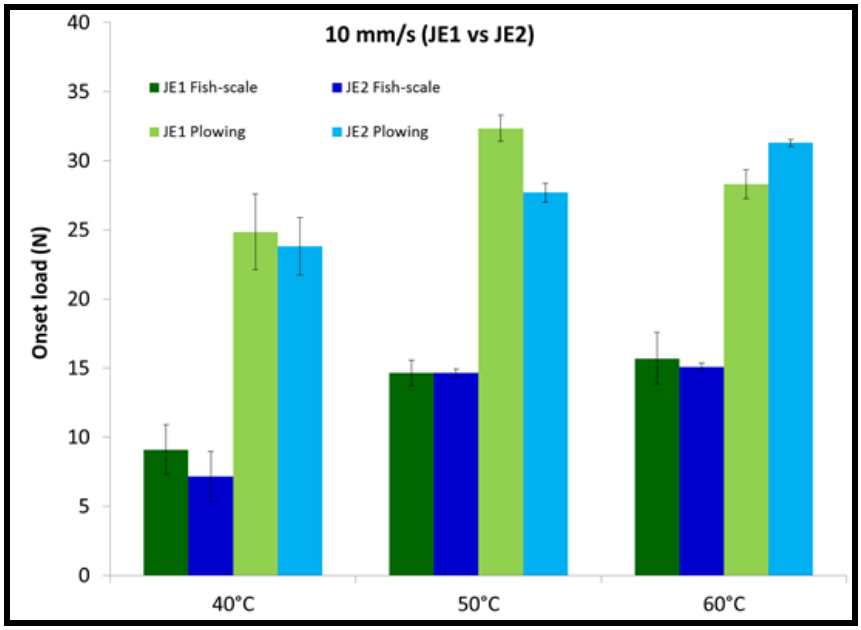

Figure 36: Onset of damage, 10mm/s, JE1 vs JE2

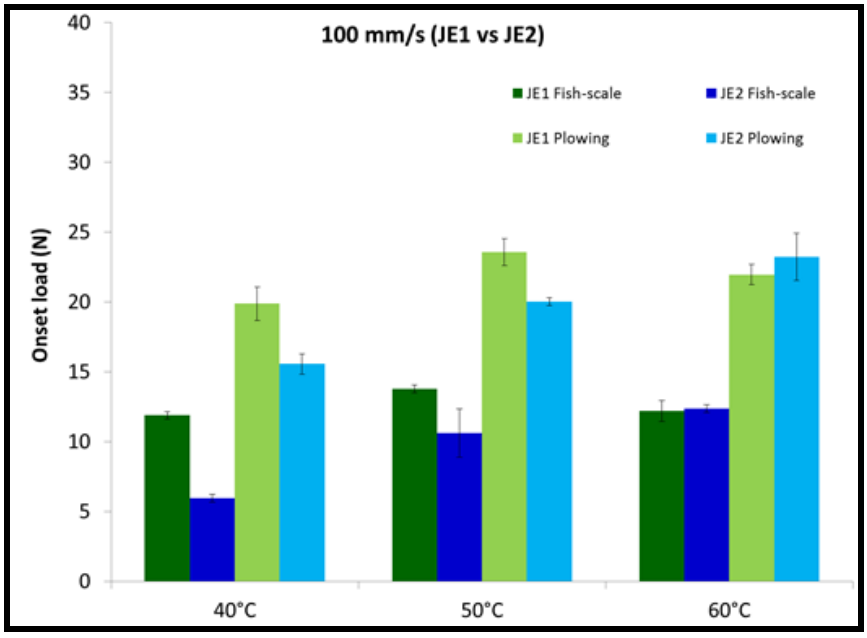

Figure 37: Onset of damage, 100mm/s, JE1 vs JE2

From figures 35, 36 and 37, it is observed that the onset of fish scale does not depend on the rate of testing. At lower mold temperature, the onset of fish scale is comparatively delayed for samples made at lower melt flow rate compared to the samples at high melt flow rate, which show the earliest onset of fish scale formation. The MFR does not have as much of a visible effect on the onset of damage of the material as it does on the onset of visibility of the material.

The onset of plowing is much more sensitive to the rate of testing than the onset of fish scale formation. At higher rates of testing, all samples show earlier onset of material removal, as expected. At 4MFR, the samples do not show any dependence of onset of material removal on the mold temperature. However, there is an observable trend in system JE2, The onset of plowing is delayed with the increasing mold temperature, especially when the rate of testing is high.

MFR has an effect on onset of visibility but no effect on the onset of fish scale or plowing. Samples show whitening at fish scale but not at the onset of fish scale, rather at a time when it is very pronounced. At high MFR, samples increasing mold temperature show delayed plowing damage. Low MFR samples are not as sensitive to mold temperature.

The surface crystallinity of the system with higher MFR increases with mold temperature. When the MFR is high, or the system has a lower molecular weight, the chains are shorter. At higher mold temperature, these chains could have more freedom of movement and align themselves better, causing a more crystalline surface layer and therefore improving scratch properties. The onset of fish-scale formation was associated

to the ultimate strength. A more crystalline surface would obviously have better hardness and ultimate strength, causing delayed onsets of both fish scale and plowing damage.

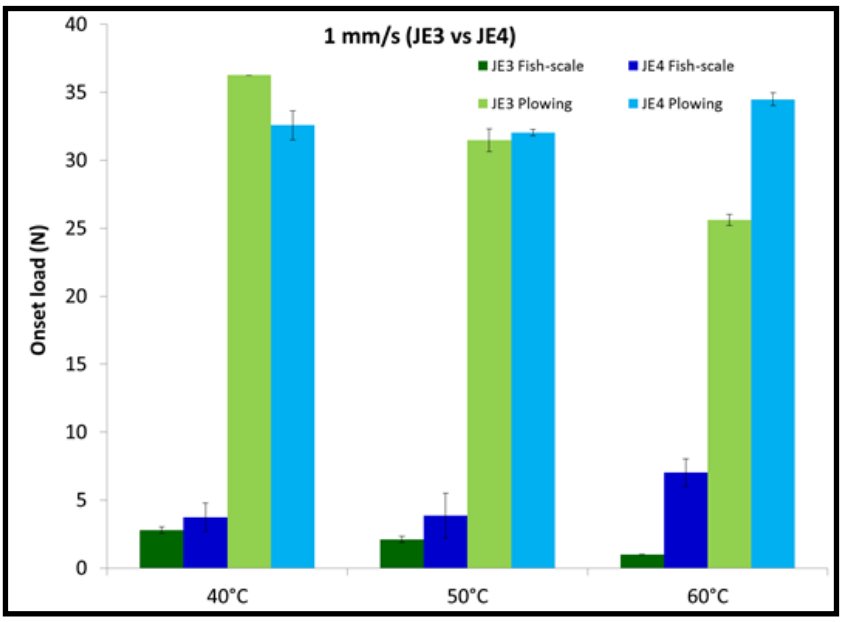

Figure 38: Onset of damage, 1mm/s, JE3 vs JE4

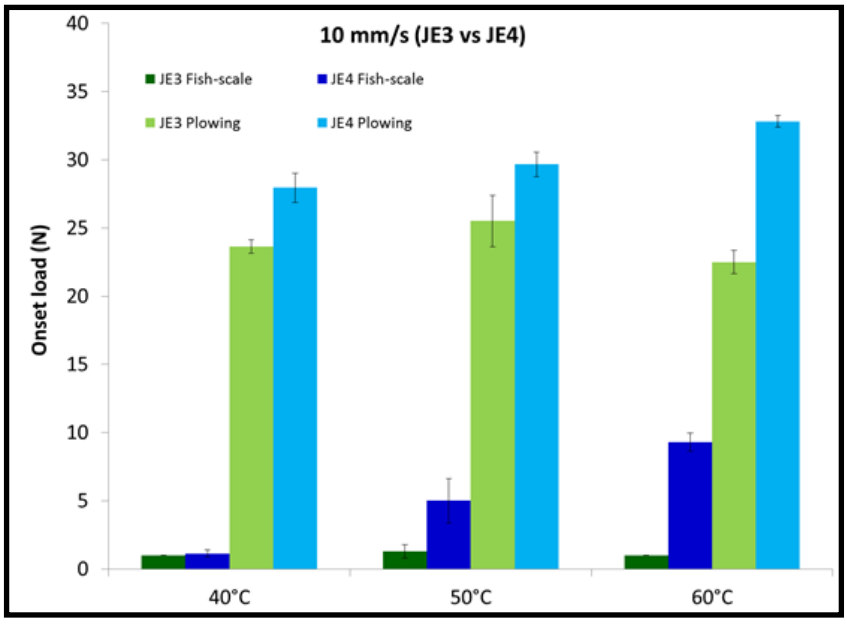

Figure 39: Onset of damage, 10mm/s, JE3 vs JE4

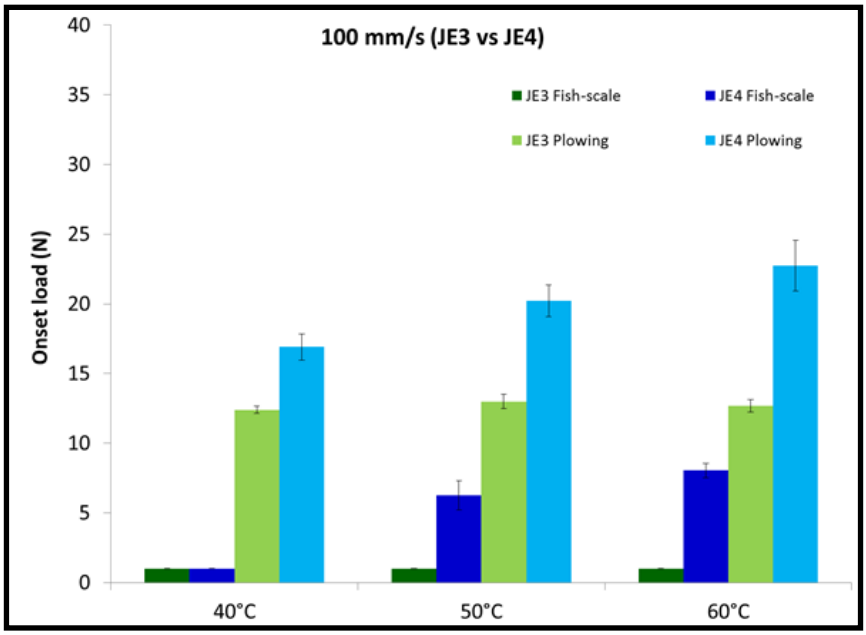

Figure 40: Onset of damage, 100mm/s, JE3 vs JE4

There is a notably early onset of fish scale formation for all scratches on the JE3 and JE4 sample systems, as seen in figures 38, 39 and 40, indicating that there is very little ironing effect or groove formation at the start of the scratch. This could mean that the samples are softer in nature compared to the JE1 and JE2 systems. As expected, the onset of plowing is initiated earlier at higher rates of testing for all samples. The effect of the scratch additive on the onset of plowing becomes more and more visible as the rate of testing is increased. There is not much of a difference in the onset of plowing damage for 1mm/s, but the scratch additive shows a visible improvement in scratch performance for tests at 10mm/s and 100mm/s.

The onset of fish-sale formation is associated to the ultimate strength of the material, and the onset of plowing includes a factor which is not involved heavily in fish

scale formation, which if the accumulation of material in front of the tip. Depending on the rate of scratch, the material removed by the tip is either passed up to the sides of the scratch or accumulates with the scratch tip. If the material is accumulated in front of the tip, there is an increase in scratch co-efficient of friction, which will be accompanied by a more severe damage. At lower rates of testing, the material removed is usually pushed to the sides of the tip, whereas at higher rates, the removed material is more likely to build up in front of the tip in the scratch path and get compressed by the tip and thereby increase tangential load on the tip. This effect is reflected in the onset of plowing damage in the above results.

Since TPOs are among the softer polymers, they exhibit lower yield stresses, and form fish scale soon. For the above samples, there is a very early fish scale formation for the JE3 system without additive. When additive is added, the friction is reduced since the additive acts as a slip agent. This causes lesser heat generated, lesser material accumulated and delayed onset of fish-sale formation and a slightly longer groove formation.

4.4: SCOF of scratch tests

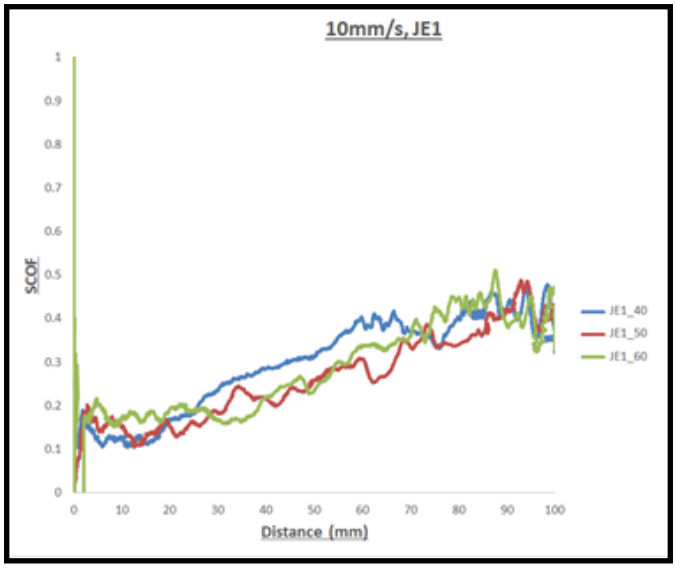

Figure 41: SCOF 10mm/s, JE1

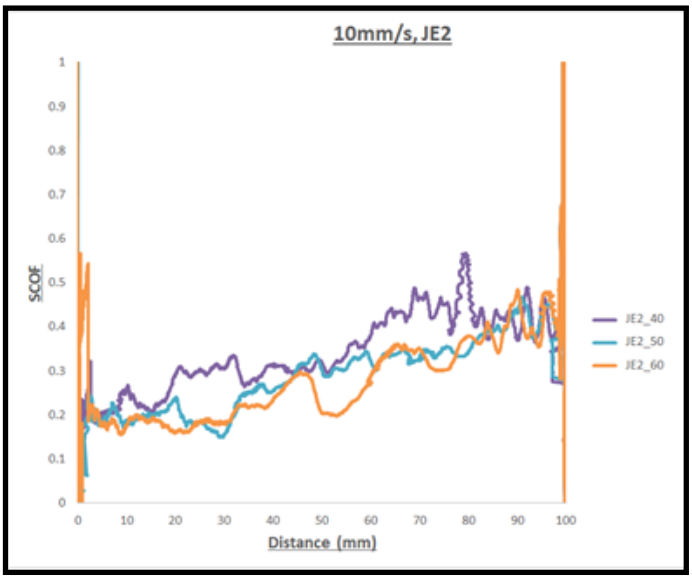

Figure 42: SCOF 10mm/s, JE2

The scratch co-efficient of friction takes into account both the surfaces in contact and the material build-up in front of the tip during the scratch process. Figures 41 and 42 show the comparison for different mold temperatures of the sample systems JE1 and JE2. The SCOF is a parameter which is usually prominent in the earlier stages of scratch. During the earlier stages of scratch, the tip has not yet reached the point to which it causes plowing and has not penetrated the surface. There is a low normal load in this stage of the scratch, which means the tip does not compress the material under it completely and thereby increase the overall area of contact. At this phase of the scratch, the damage done is on the surface as opposed to deeper plowing damage. The virgin undamaged surface roughness of the samples can be associated to SCOF at this part of the scratch.

It has been established that the mold temperature's increase does not have a very visible or significant effect on the system with low MFR. The scratch co-efficient of friction graphs for all three rates of testing, 1mm/s, 10mm/s and 100mm/s all point to this fact. For samples JE1, as expected, there is no variation of SCOF with change in mold temperature. The SCOF is not very differentiable since mold temperature does not show a strong effect when the system has a low MFR. In the case of the higher MFR system JE2, however, the SCOF curves reflect the visibility analysis results, especially at the start of the scratch along the first few millimeters. The lower mold temperature system shows higher SCOF values and earlier onset of visibility and damage.

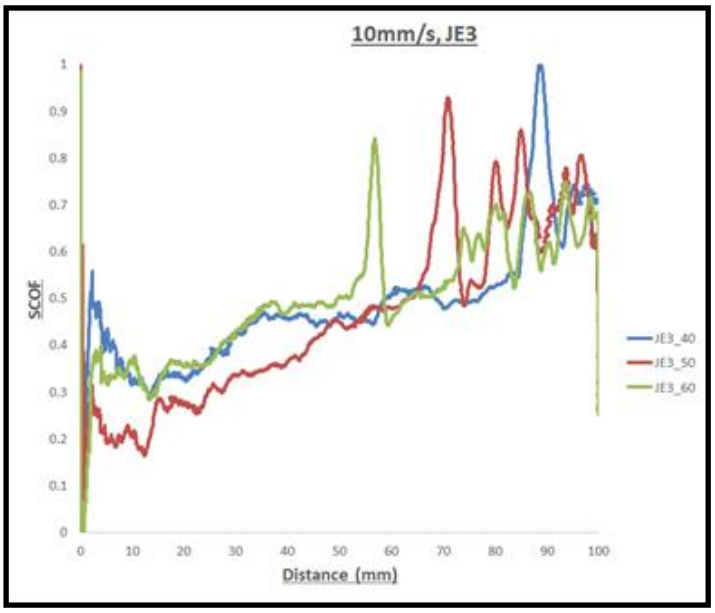

Figure 43: SCOF 10mm/s, JE3

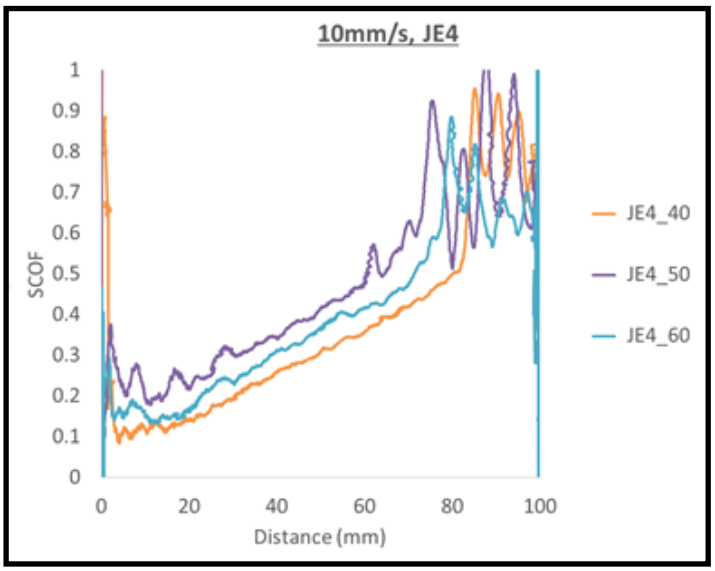

Figure 44: SCOF 10mm/s, JE4

The material of systems JE3 and JE4 is softer compared to the systems JE1 and JE2. Therefore, there is much more depth of penetration and much higher SCOF observed in the case of these systems. In Figures 43 and 44, there are sharp peaks on the SCOF curves and large increase in slope towards the ends of the scratch which correspond to plowing damage. The tip digs into the material and there is much higher tangential resistance force against the direction of scratch.

As observed in the case of the onset of visibility and damage, there is no significant effect of mold temperature on the SCOF of the TPO system without scratch additive. The system with scratch additive, system JE4 shows a much clearer trend. As the mold temperature increases, there is more slip agent presence on the surface of the material, which gives a lower SCOF to the system.

5. MAR TESTS

5.1: Mar testing criteria

Mar tests are superficial in comparison to scratch tests and are not expected to show nearly as severe material removal damage as scratch tests. Mar tests are done with tips that cause area damage as opposed to a single-line damage of a scratch tip. A Self-adjusting barrel tip, as shown in Figure 45, was used for the mar testing of samples within a load range of 1-120N at a testing rate of 10mm/s.

Figure 45: Self-adjusting barrel tip

The self-Adjusting barrel tip is a tip that has been known to cause ironing type of damage i.e., it tends to smooth the surface by “ironing out” peaks and valleys. This is because the tip itself is very smooth and hard. The self-adjusting nature of the tip also

makes it such that the tip has a degree of freedom to get tilted by a small angle perpendicular to the direction of mar during testing. This makes material removal unlikely and gives rise to an “ironed” mar area.

The type of mar which is more likely to occur to polymeric components during real world use is a roughening type of mar. It can be seen when two surface scrape against each other. Even if one of the surfaces is rough, there is a roughening type of effect on both surfaces as a result of this type of contact. To emulate this type of mar, one test was done on each plaque using a square tip with a polishing surface of cloth at a load range of 1-30N. The cloth tip, as shown in Figure 46, causes a roughening type of damage as opposed to the barrel tip’s ironing damage.

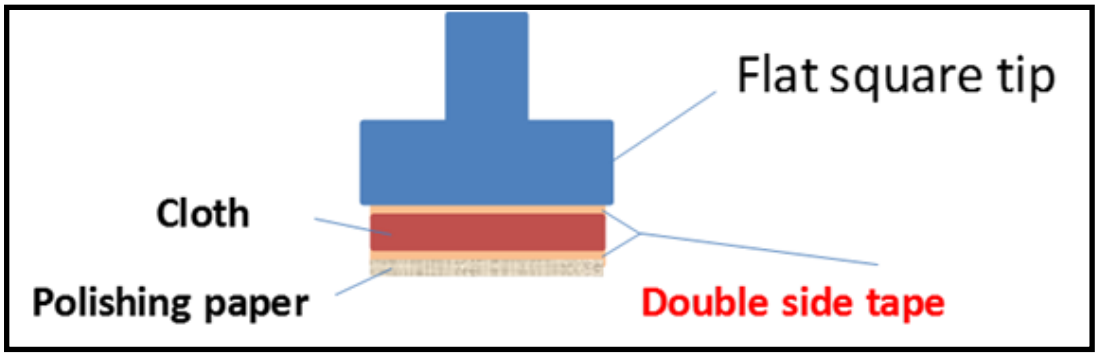

Figure 46: Schematic of a cloth-covered mar tip

Mar damage by both types of tips were imaged using a DSLR camera in a dark room under a single light source under fixed conditions as shown in Figure 47 and analyzed using the ASV© software. The aspect of mar damage which is focused upon is visibility, since mar does not cause nearly as severe mechanical damage as scratch.

Previous work suggests that the onset of visibility is not the factor which decides the severity of mar damage, but the degree of visibility of mar as a whole, which is expressed in terms of a Contrast%. The contrast percentage of each section along the length of the mar is shown in the form of a contrast curve, which can be used to compare the overall visibility of mar.

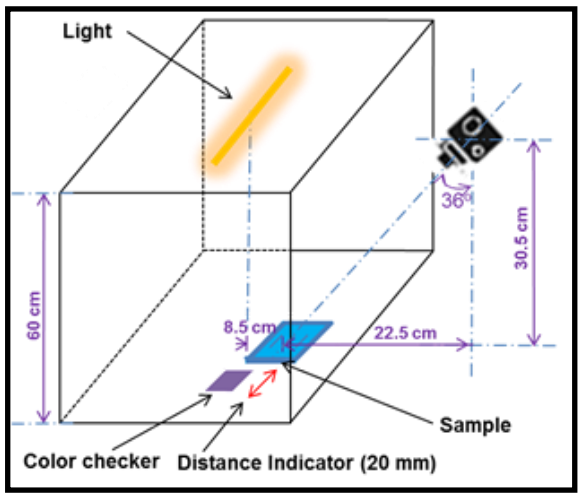

Figure 47: Setup for imaging and human observation

As with scratch tests, three human observers were also asked to give their views on the visibility of mar. Since the onset of visibility of mar is not a point of priority, observers were asked to rate the samples on the degree to which they were visible. Observers were allowed to view the mar under the same lighting conditions as was used for imaging and asked to rank samples based on visibility. Although this is not a quantitative approach, it can be used to establish whether or not the Contrast curves obtained by ASV analysis are credible and relate to actual human observation. SCOF is

also used as a tool to explain the mar behavior of sample systems, since mar is a surface phenomenon. As previously stated, it is the ratio of the tangential resistance force experienced to the normal load applied by the tip on the sample plaque. The difference between the SCOF and co-efficient of kinetic friction is the effect due to any build-up in front of the tip which adds to the resistance experienced during the test. It can easily be deduced that as the extent of material build-up in front of the tip varies along the length of testing, therefore, unlike the co-efficient of kinetic friction, SCOF is a variable quantity and needs to be plotted along the length of test.

5.2 Mar test visibility- contrast curves

Mar damage is much more superficial than scratch damage. It is the difference in the geometry of the mar tip and scratch tip, and the topography of the polishing surface which dictates how severe the mar damage inflicted on a sample would be. As the surface roughness and hardness of the tip increase, the type of damage induced on the specimen being tested will drift towards a scratch type of damage. Therefore, using a very hard and rough tip would cause a mar which would have a scratch-like material removal effect on soft specimens and cracking damage on hard specimens.

A self-Adjusting barrel tip is used to conduct all mar tests on samples. This tip is smooth and has a small degree of freedom to negate any tilt while fixing the tip which could damage one side of the mar in a different way from the rest of the mar area. This

type of irregular marring is known as the “edge effect” and has been observed in mar made by rigid tips.

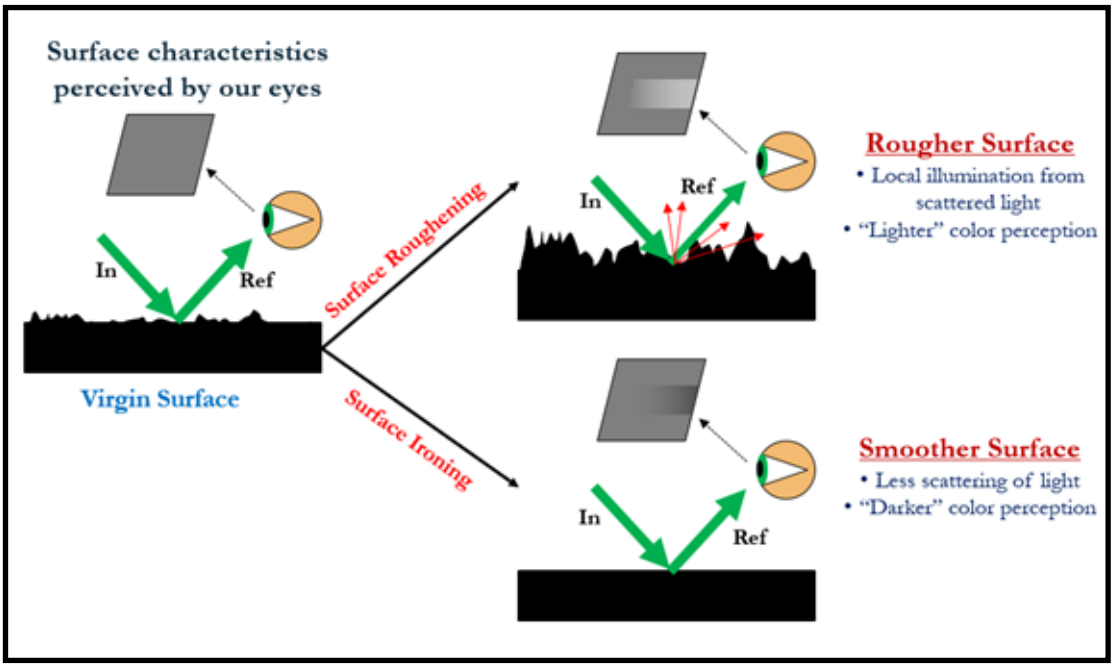

Figure 48: Perception of smoother and rougher surfaces [38]

As demonstrated in Figure 48, when a beam of light strikes a perfectly smooth surface, the entire beam of light is reflected at an angle of reflection which is equal to the angle of incidence. But since there is no perfectly smooth surface in nature, not the entirety of the beam of light is reflected in the same direction. A part of the beam incidents on surface irregularities and gets reflected at other angles. This phenomena in which a part of the incident beam is lost is called diffusive reflection. When mar damage is done to the surface the amount of diffusive reflection increases or decreases depending on whether the surface has undergone a reduction or an increase in surface roughness,

which directly translates to an increase or decrease in the number of irregularities which cause light to undergo diffusive reflection.

Since the contrast curve and contrast percentage rely on formulae which compare the intensities of the light from the marred region to the surrounding virgin surface, if the marred region is darker, there will be a negative contrast observed in the contrast curve, and vice-versa.

As stated earlier, human observers were asked to rank the samples in terms of the extent of visibility of mar. Although this is not a quantitative measurement, it is a good tool for comparison of the results since imaging of mar is subject to many variables and has a lot of scope for error.

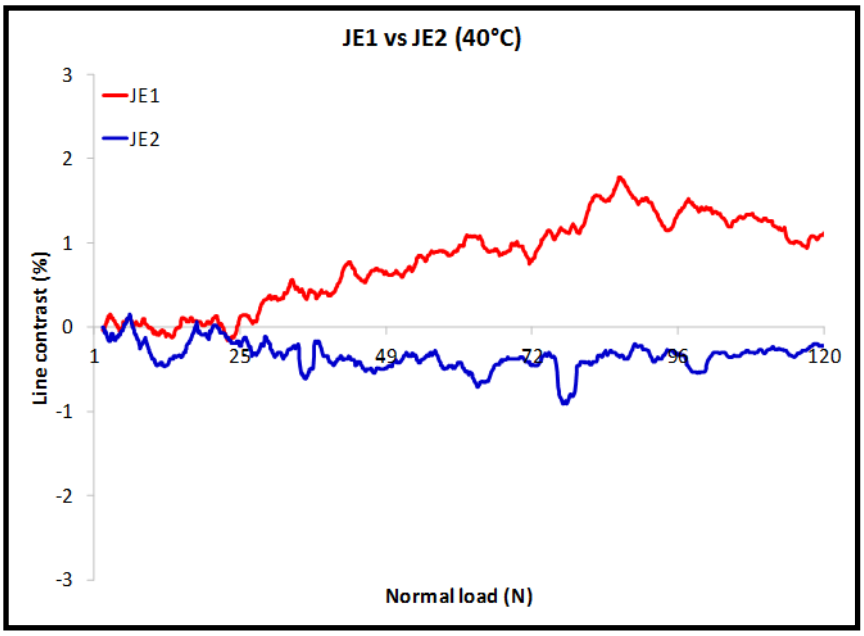

Figure 49: Contrast curve, JE1 vs JE2, 40 degrees Celsius

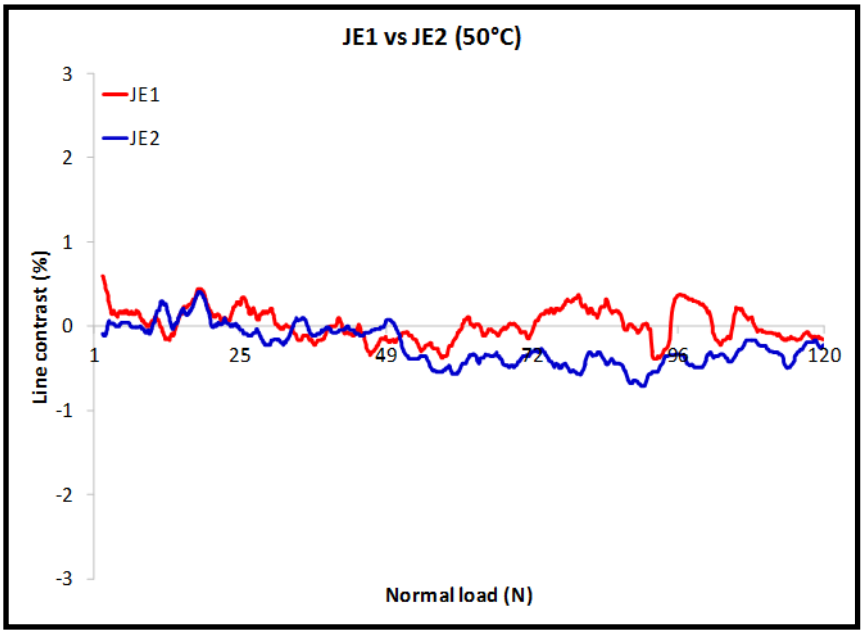

Figure 50: Contrast curve, JE1 vs JE2, 50 degrees Celsius

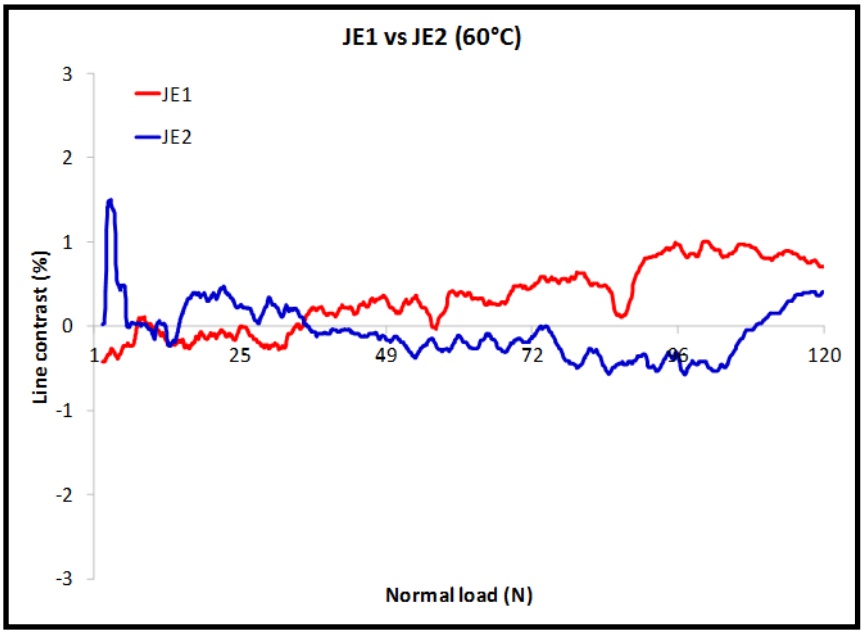

Figure 51: Contrast curve, JE1 vs JE2, 60 degrees Celsius

From Figures 49, 50 and 51, Sample Systems JE1 and JE2 do not exhibit heavy mar damage at all when tested with a barrel tip. Even when allowed the freedom to tilt the sample and view them for comparison, human observers claimed that the marred area on the samples was only vaguely different from the undamaged area. However, they stated that marred region on the JE1 system was more visible than the marred region of the corresponding sample of the JE2 system.

The contrast curves obtained after the ASV analysis of the samples offer an explanation to the human observers' statements. The contrast curves of system JE1 and JE2 show very low contrast percentages, not greater than 2% or less than -2%. Since the human eye only easily perceives a contrast of over 3%, it is understandable why observers had a hard time judging the mar of the samples. The JE2 sample system contrast curves are mostly near-zero negative values, which indicate that there is only a mild darkening of the sample even at loads as high as 120N using the barrel tip. In comparison, the JE1 samples also show very low contrast% values but these values are higher than the corresponding JE2 curves. Thus, both the ASV and human observers are in agreement that the system JE1 shows a slightly more visible mar compared to the JE2 system.

To obtain a different type of mar damage which could separate these systems, tests are done using a cloth tip on the JE1 and JE2 samples. Since this type of tip is much rougher than the smooth steel barrel tip, the applied load need not be very high to obtain visible damage. A load range of 1-8N is applied using the cloth tip to study the mar behavior.

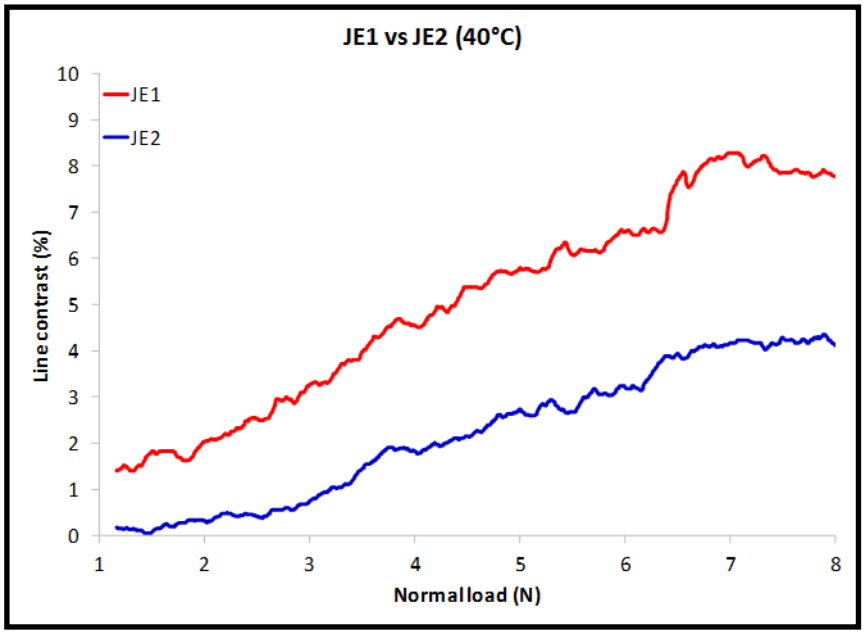

Figure 52: Cloth tip contrast curve, JE1 vs JE2, 40 degrees Celsius

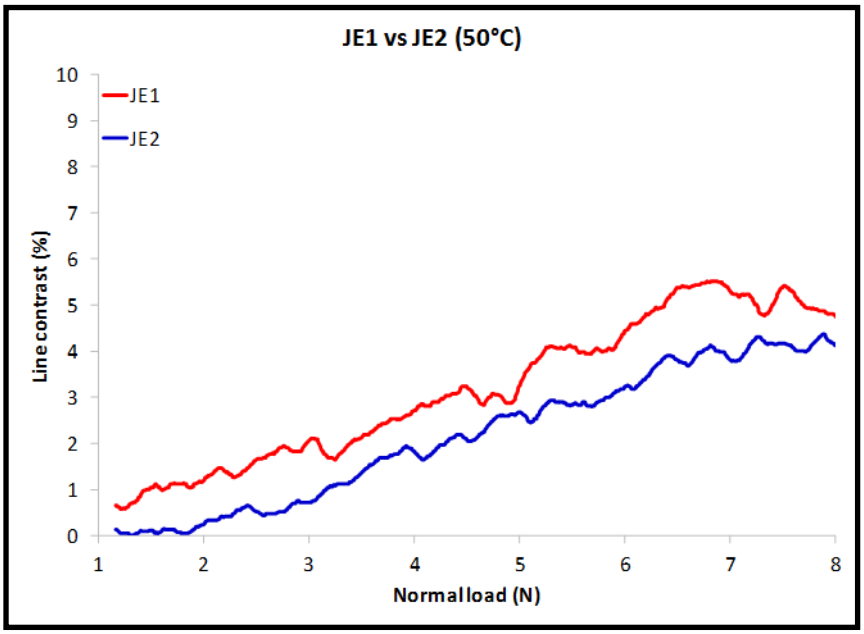

Figure 53: Cloth tip contrast curve, JE1 vs JE2, 50 degrees Celsius

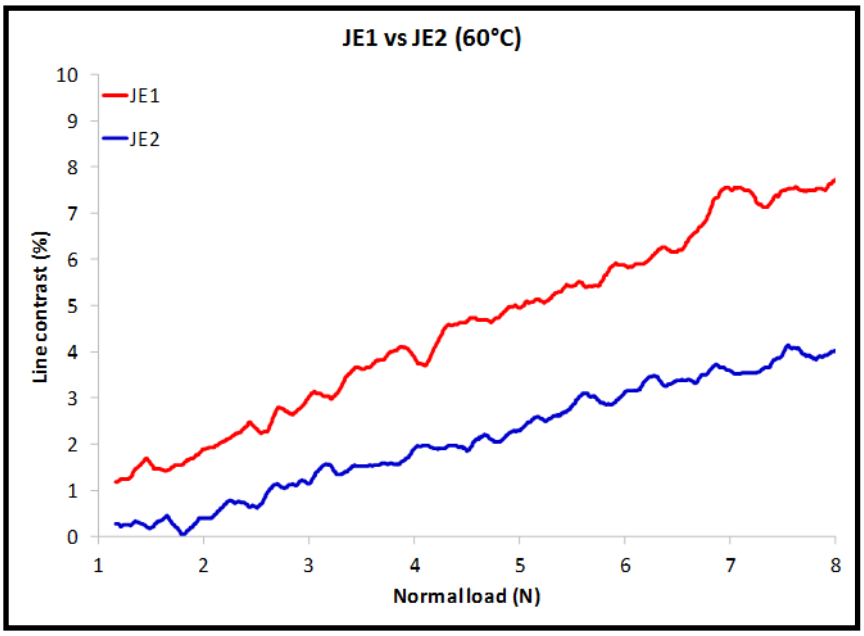

Figure 54: Cloth tip contrast curve, JE1 vs JE2, 60 degrees Celsius

The mar done using a cloth tip was much more easily perceived by human observers. According to them, system JE1 had more visible mar damage compared to system JE2. The contrast curves obtained by ASV analysis of the cloth tip tests, given in Figures 52, 53 and 54, show a much wider gap between the systems than in the case of barrel tip tests. Firstly, the Contrast% values are all positive, which indicates whitening or roughening of the surface. The JE1 system exhibits higher contrast% than system JE2.

In terms of ranking between different mold temperatures for each sample system, for both systems JE1 and JE2, human observers ranked Barrel tip mars on the 40˚c samples as the most visible, followed by 50˚c and 60˚c. However, the contrast curves at all three temperatures are very similar. System JE1 shows most visible mar damage on the sample molded at 40˚c, in the case of both barrel tip and cloth tip, which is in

agreement with the human observation results. The JE1 samples show better scratch behavior and the JE2 samples show better mar behavior. In previous work done, it had been shown that decreasing the lower MFR injection molding processes give PP which has a higher skin layer thickness [39] Since molecules higher MFR and higher mold temperature have better freedom to align and orient themselves on the surface, they form a more crystalline layer than the lower MFR system. The scratch damage of fish-scale and plowing depends on the strength of material but since mar is much more superficial, the alignment of molecules on the surface has a much more pronounced effect and therefore, the mar on the system with higher MFR is less visible compared to the higher MFR system. A load range of 1-120N was applied using a self-adjusting barrel tip on all samples to create a marred region. Again, a time interval of at least 48 hours was allowed for these samples before imaging and ranking by human observers.

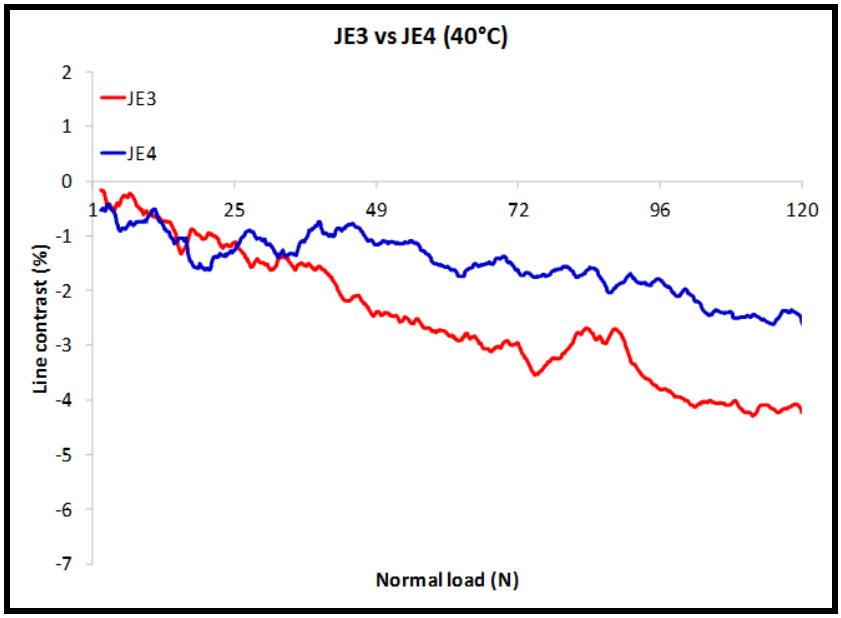

Figure 55: Contrast curve, JE3 vs JE4, 40 degrees Celsius

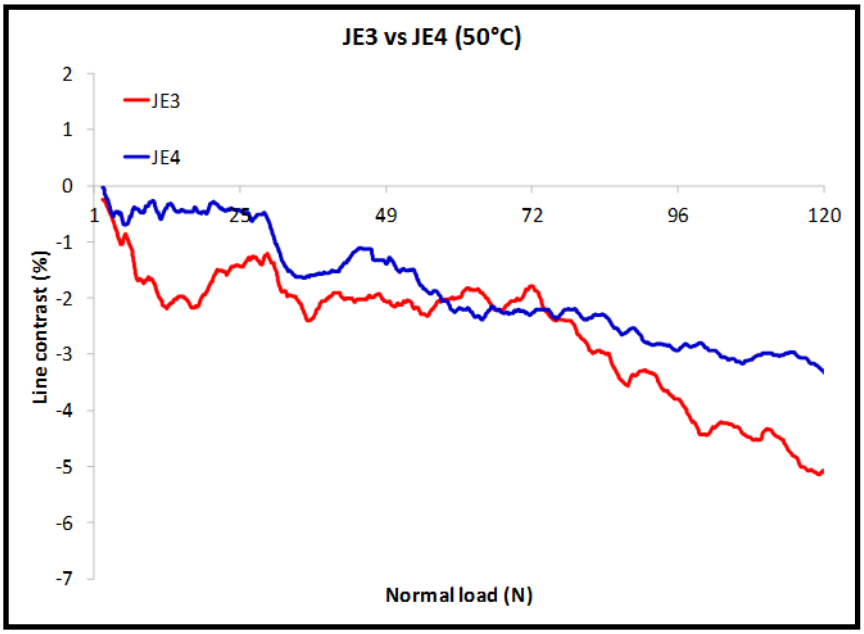

Figure 56: Contrast curve, JE3 vs JE4, 50 degrees Celsius

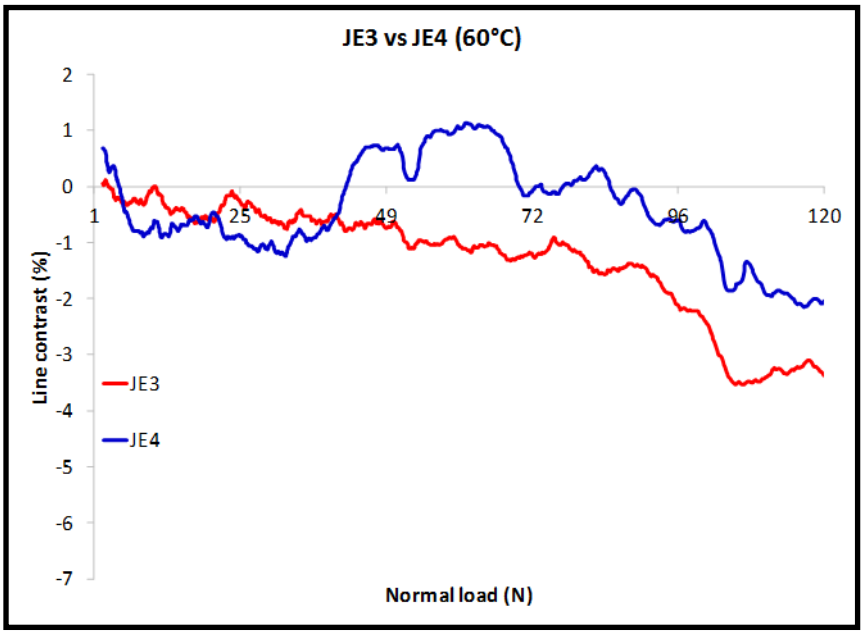

Figure 57: Contrast curve, JE3 vs JE4, 60 degrees Celsius

From Figures 55, 56 and 57, it is clear that the self-adjusting barrel tip caused a much more easily visible mar to the JE3 and JE4 samples compared to the JE1 and JE2 samples. The mar on the JE3 and JE4 samples caused by the barrel tip is darker compared to the virgin surface. Human observers felt that the mar on the JE3 samples was more visible than mar on the JE4 samples for each corresponding mold temperature. On imaging and performing the contrast curve analysis using the ASV software, the contrast curves obtained show negative contrast percentage values which support the view of darkening and ironing of samples and also, the curve of the JE3 samples has a more negative trend to it than the JE4 samples contrast curve.

Human observers ranked the 40°c samples to have the most visible mar damage, followed by 50°c and 60°c, for both system JE3 and JE4. They also said that the mar looked almost the same and that there was not much of a difference. From the contrast curves, it is almost impossible to differentiate between the three different mold temperatures, except in the case of JE4, where the mar at 60°c shows a contrast curve which is not as unidirectional as the rest of the curves.

Mar mostly happens due to the change in surface roughness of the sample, the slip agent layer on the surface causes the mar tip to slide over the surface and not cause as much roughness change as would have otherwise occurred without its presence. Also, the presence of more slip agent on the surface with increasing mold temperature causes higher mold temperature samples to exhibit lower contrasts and lower visibility, as was in the case of scratch tests. Although the tests conducted using the self-adjusting barrel

tip produces visible mar and differentiable results, the cloth tip was also used to induce mar damage on JE3 and JE4 samples at load ranges of 1-8N.

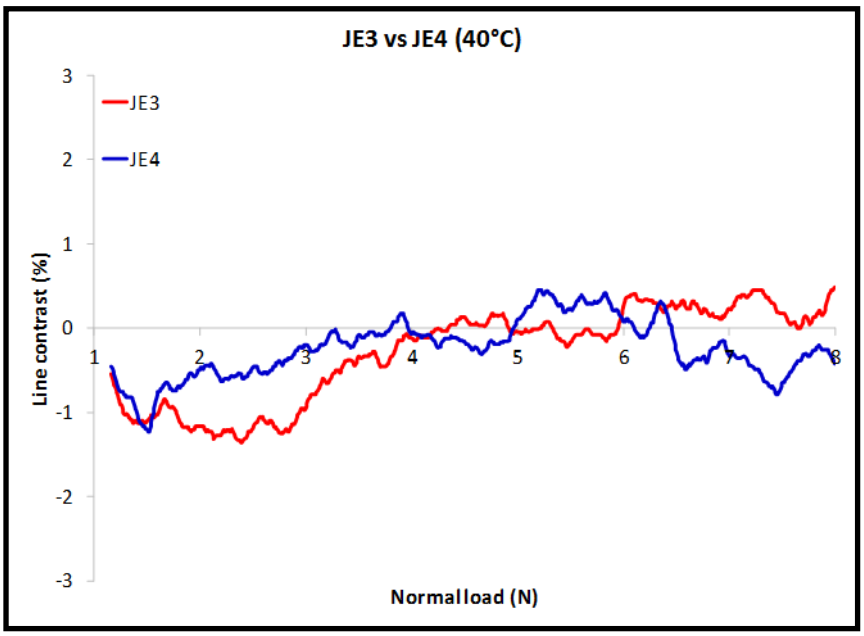

Figure 58: Cloth tip contrast curve, JE3 vs JE4, 40 degrees Celsius

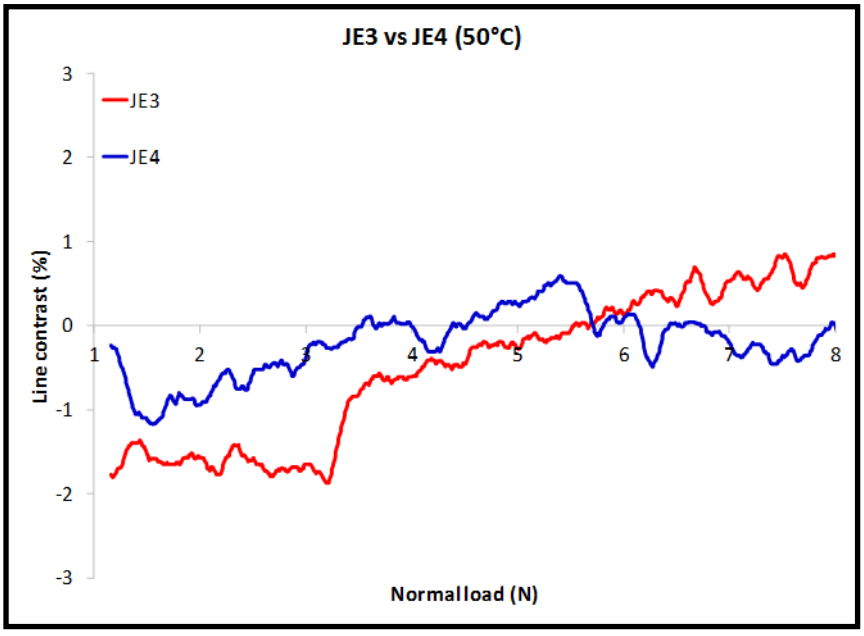

Figure 59: Cloth tip contrast curve, JE3 vs JE4, 50 degrees Celsius

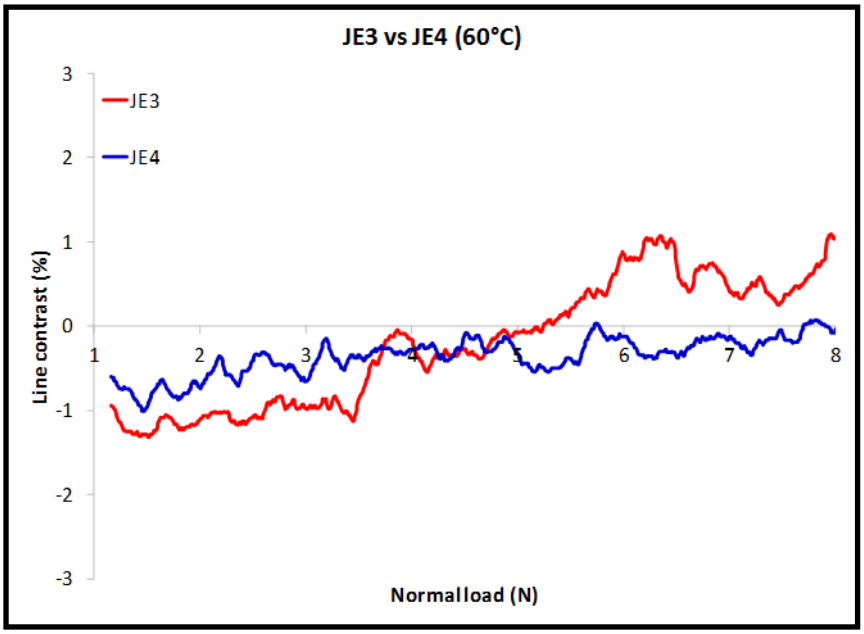

Figure 60: Cloth tip contrast curve, JE3 vs JE4, 60 degrees Celsius

The mar damage caused by the cloth tip on the JE3 and JE4 samples was less visible compared to the damage caused by the barrel tip, as seen in Figures 58, 59 and 60. In samples of all three mold temperatures, the sample system JE3 endured more visible mar damage compared to system JE4. The nature of this damage on the samples is also different, in the sense that the marred region appears darker than the virgin surface at some parts at some angles and the same region appears brighter and whiter than the background virgin surface at other angles. The contrast curve analysis produces results which show low contrast% values, suggesting low visibility of mar. There are parts of the contrast curve which lie above the X-axis and below the X-axis, which supports that there are regions which are both darker and whiter than the virgin surface on the path of the same mar. Also, neither of the three mold temperatures' graphs show a

significantly higher or lower set of contrast% values or a steep or deep curve, which suggests they are all not very differentiable.

Since the TPO material is soft, the asperities on the surface are ironed out initially. As the load applied by the cloth tip increases, the two surfaces come into contact with each other with a much higher contact area and compressive force, and the cloth tip causes roughening damage. The graphs are tough to differentiate in terms of contrast% and no conclusions can be drawn from the tests done using the cloth tip on the JE3 and JE4 samples.

5.3: LSCM- surface roughness change due to mar

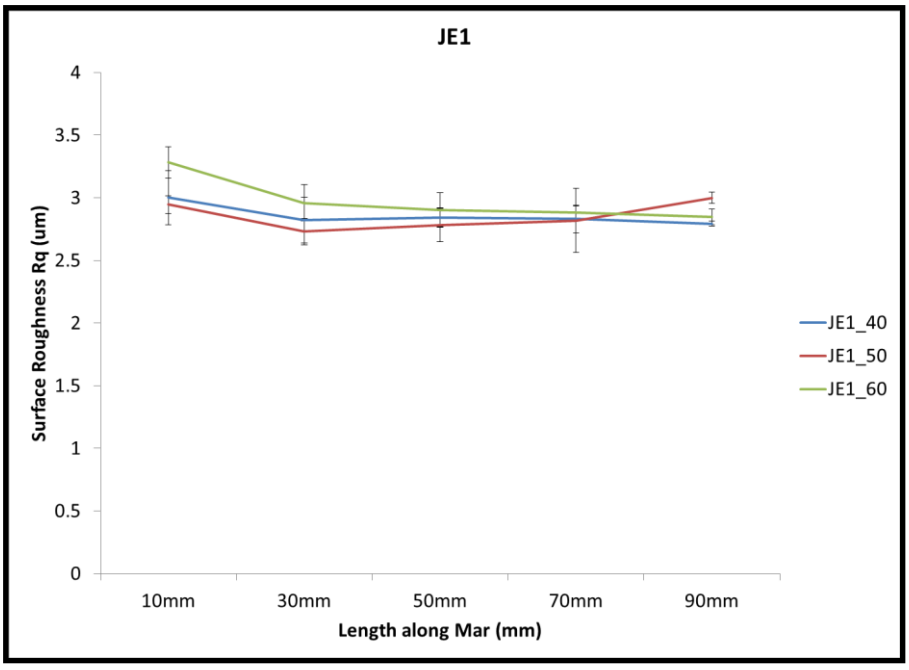

Figure 61: Surface roughness (Rq), system JE1

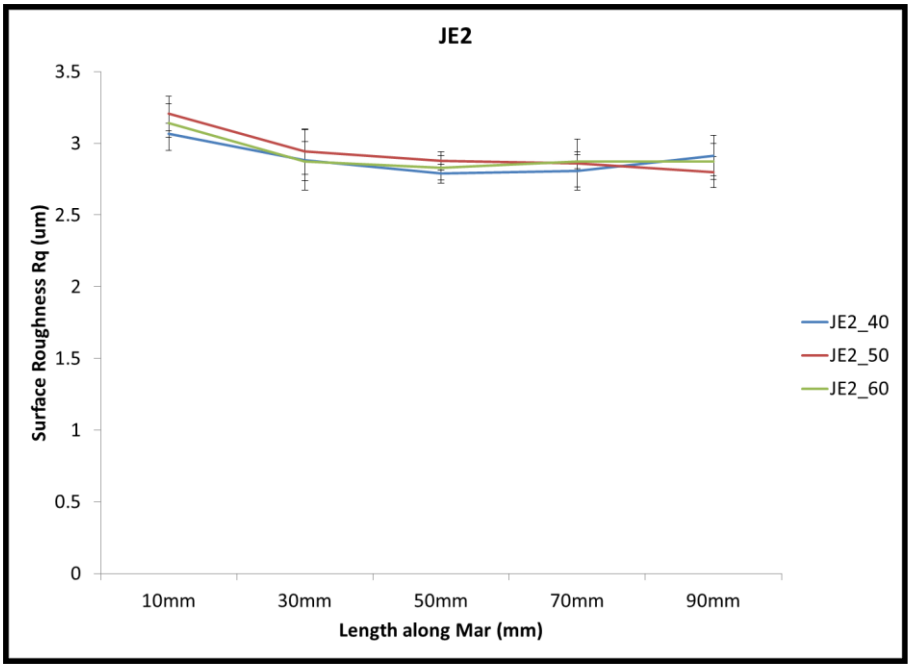

Figure 62: Surface roughness (Rq), system JE2

The surface roughness (Rq) was found using the LSCM at 10x magnification along the length of mar. The virgin surface roughness of all JE1 and JE2 samples falls between 3±0.2um. From Figures 61 and 62, it is observed that the barrel tip causes a reduction in the surface roughness along its length of mar, suggesting an ironing type of mar for all samples. But, no clear pattern is observed among mar on samples of the same system molded at different temperatures. Therefore, it can be said that mold temperature does not influence ironing mar behavior of the PP plaque samples.

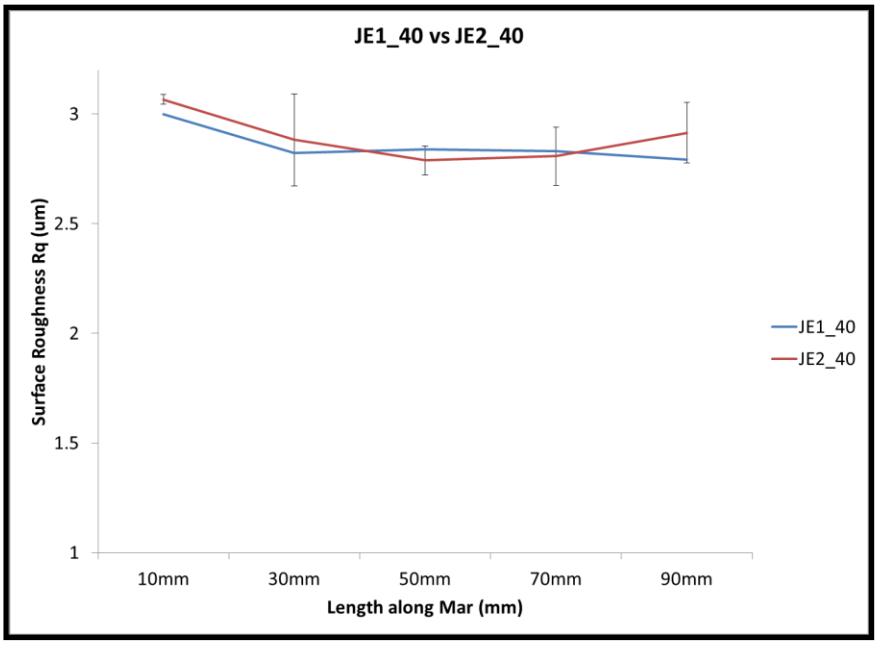

Figure 63: Surface roughness (Rq), JE1_40 vs JE2_40

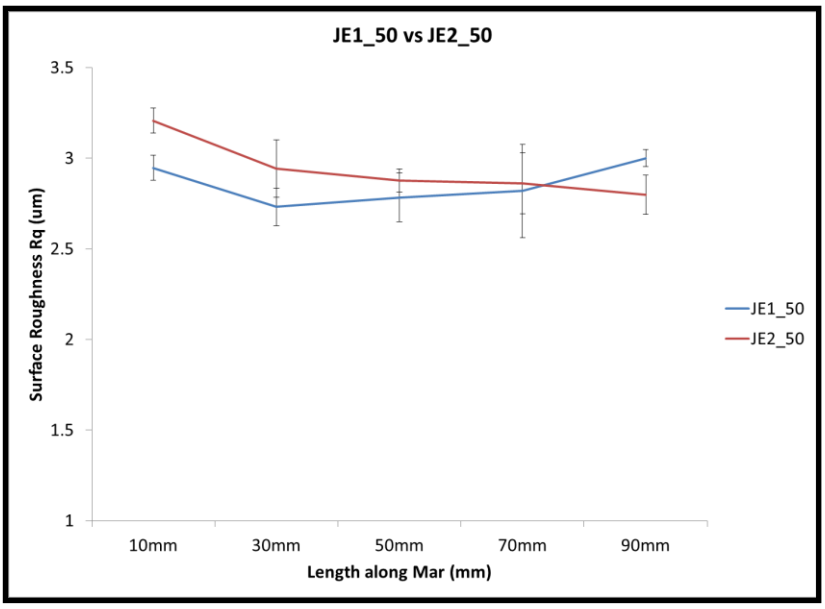

Figure 64: Surface roughness (Rq), JE1_50 vs JE2_50

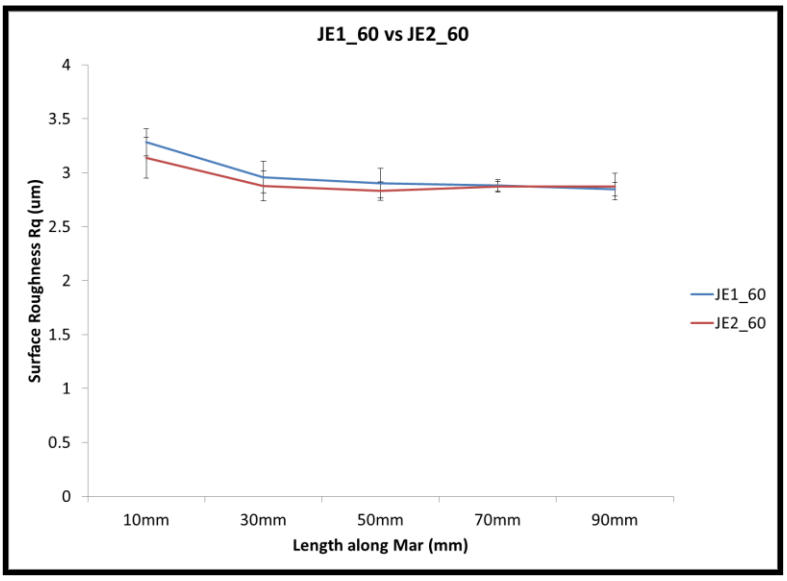

Figure 65: Surface roughness (Rq), JE1_60 vs JE2_60

To understand the effect of MFR on the surface roughness change due to barrel tip, the surface roughness of individual temperature is separately compared, and again, there is no clear common trend in the graphs in Figures 63, 64 and 65. In some cases, the low MFR system undergoes greater surface roughness change, and in other cases, it is the opposite. The only conclusion from these graphs is that the MFR does not affect the ironing mar on these samples greatly.

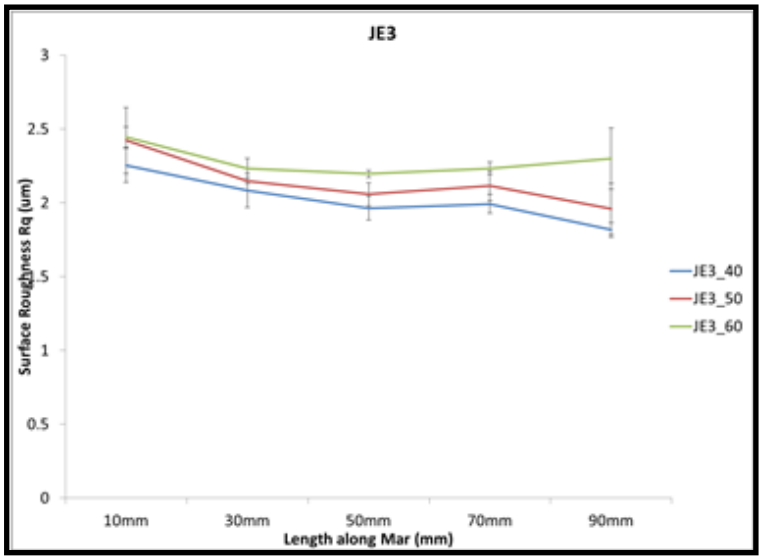

Figure 66: Surface roughness (Rq), system JE3

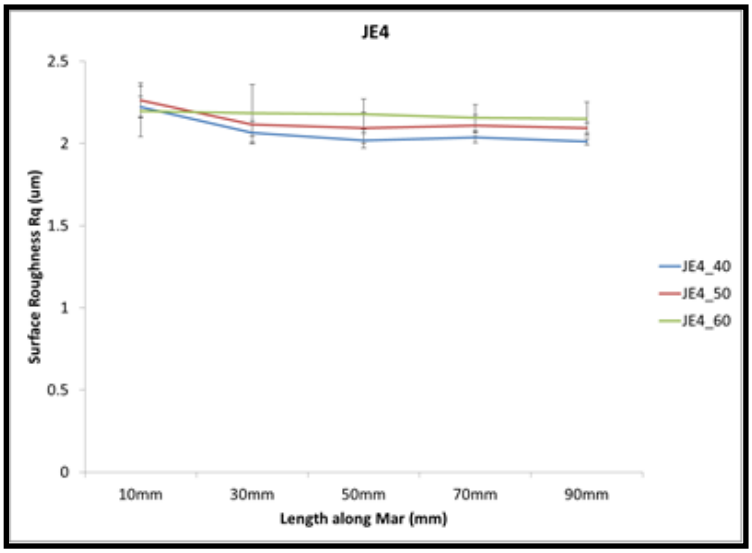

Figure 67: Surface roughness (Rq), system JE4

The LSCM results for surface roughness are again used to quantify the surface roughness change in the systems. From Figures 66 and 67, for both TPO systems JE3 and JE4, there is a visible trend in surface roughness change along the length of mar.

The samples molded at 60˚c show lower surface roughness reduction due to barrel tip mar than 60˚c, and surface roughness change for 50˚c is greater than for 40˚c. This happens for both systems, so it can be concluded that higher mold temperature makes the surface more resistant to roughness change by an ironing barrel tip.

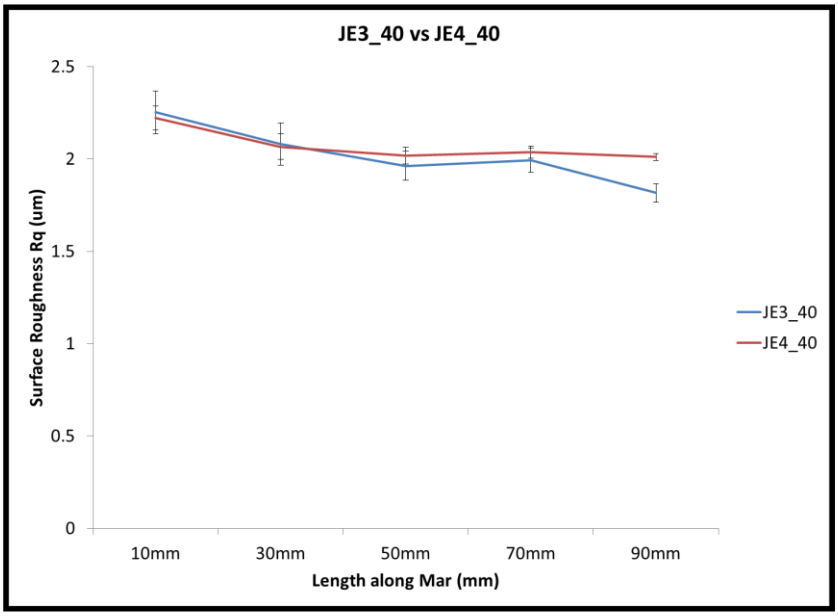

Figure 68: Surface roughness (Rq), JE3_40 vs JE4_40

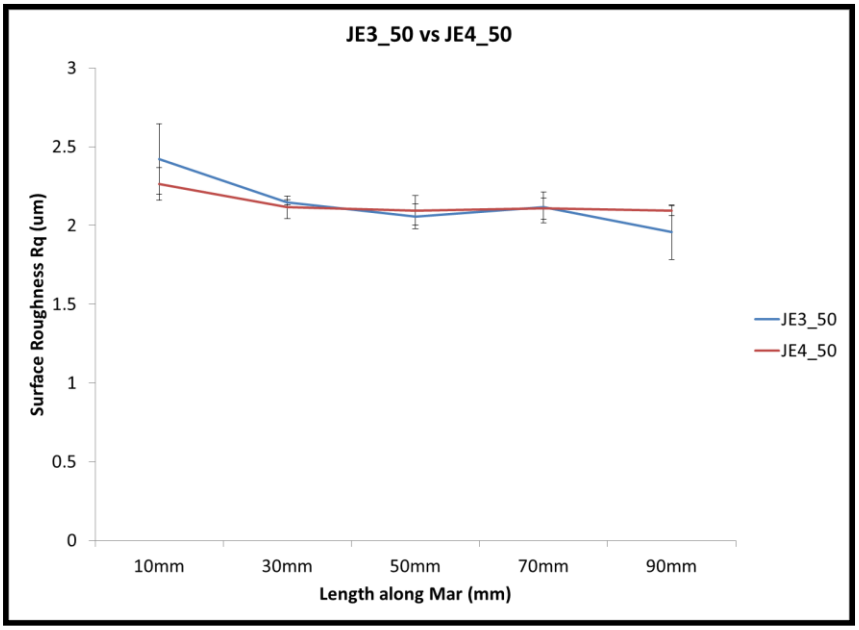

Figure 69: Surface roughness (Rq), JE3_50 vs JE4_50

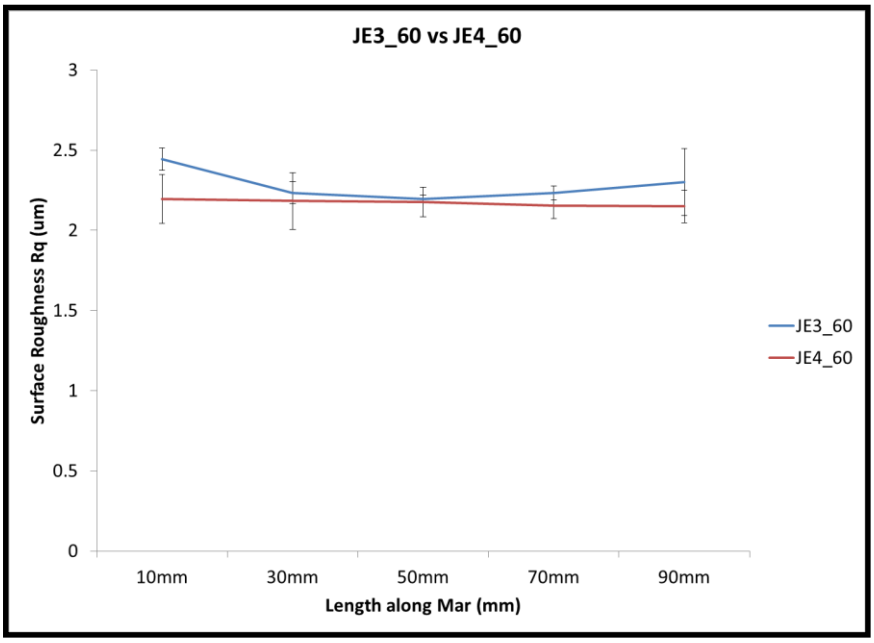

Figure 70: Surface roughness (Rq), JE3_60 vs JE4_60

The scratch additive makes the tip slide over the surface without causing as much roughness change as would have been without an additive. This is visible in the Figures 68, 69 and 70, where for all mold temperatures, samples with scratch additive on the surface show a more uniform surface roughness curve compared to the samples without additive.

5.4: SCOF of mar tests

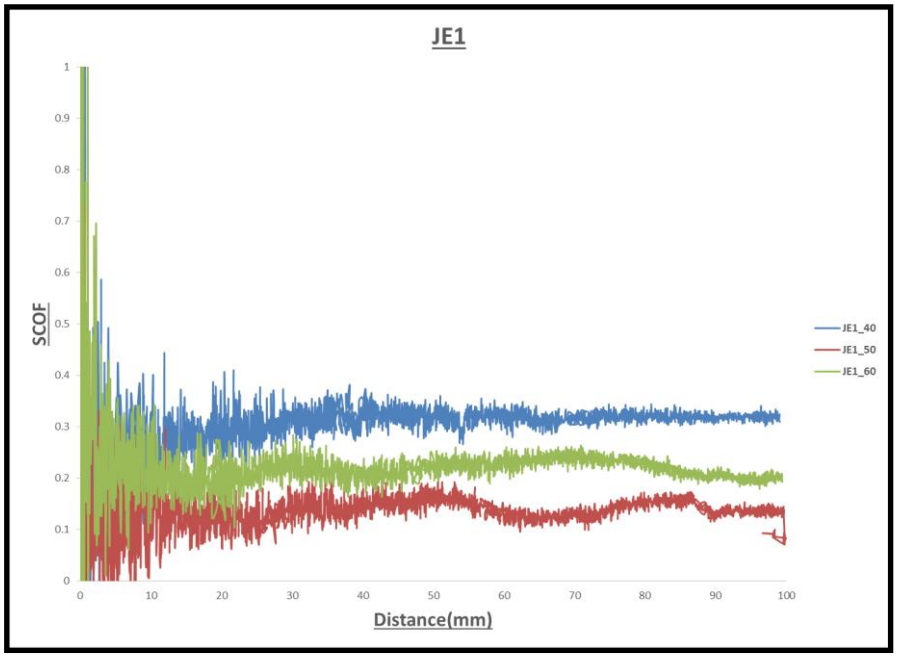

Figure 71: Mar SCOF, system JE1

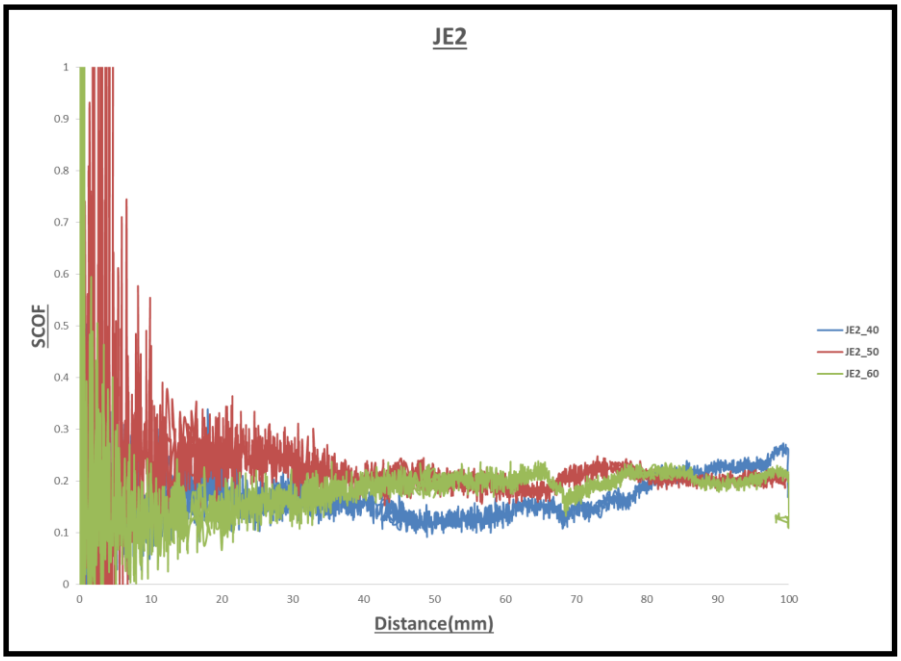

Figure 72: Mar SCOF, system JE2

The Scratch co-efficient o friction is plotted for the mar tests on the samples along the length. Since three tests were carried out with the same testing parameters for each sample, one of the three was chosen as a representative. It was confirmed that the three curves are nearly the same in all ways, before selection. From the SCOF curves for JE1 and JE2 are very different although mar behavior is not very easily differentiable. From Figure 71, System JE1 shows different SCOF for different mold temperatures, but this difference in SCOF is not reflected in the visibility or surface roughness change on the sample. It is also noted that the sample at mold temperature of 50˚c shows the least value of SCOF for system JE1 so it must have the least roughness change, and therefore, least visibility. However, this is not the case. For system JE2, however, in Figure 72, the SCOF curves are in support of the mar visibility behavior exhibited by the samples. For

all mold temperatures, the SCOF between the tip and surface along the length is nearly 0.2.

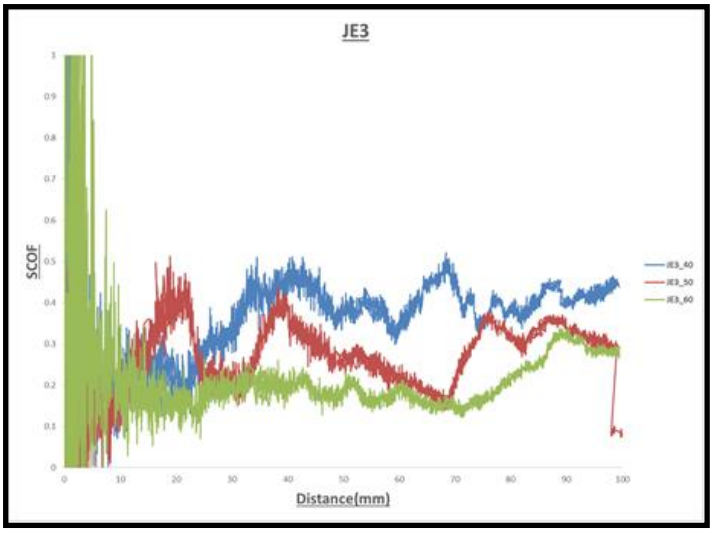

Figure 73: Mar SCOF, system JE3

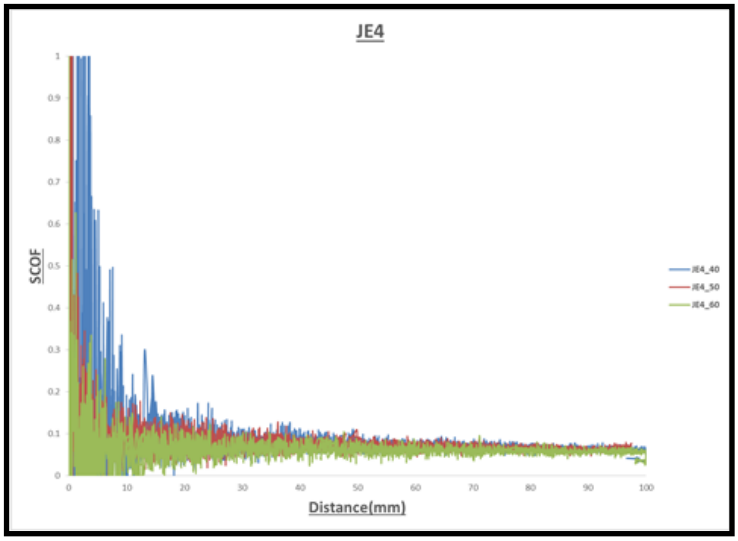

Figure 74: Mar SCOF, system JE4

The SCOF curves for the JE3 and JE4 samples in Figures 73 and 74 respectively reflect and explain the mar behavior better than in the case of the JE1 and JE2 samples. The TPO system without additive has a higher visibility and contrast% than the corresponding sample with additive. From the SCOF curve, it is seen that the friction between the surfaces is also much higher for samples without scratch additive. The mar behavior, however, improves with increasing mold temperature in the case of the sample without additive. The friction experienced by the tip as it moves along the surface is visibly lower in the case of JE3 samples of a higher mold temperature. In comparison, the JE4 samples all show very low SCOF values, which are almost the same and in each case, much lesser than the corresponding JE3 sample.

The spikes on SCOF curves of the JE3 system indicate areas of high friction. The SCOF plot is in agreement with the human observers' assessment of the higher mold temperature mar being the least visible, and with the LSCM outcome that there is much more surface roughness in the system without additive than in the system with additive. The low SCOF explains why there is less change in surface roughness of the JE4 system and also explains the improved mar visibility compared to system JE3. The increasing effect of the scratch additive with increasing mold temperature is not very visible in the SCOF curves of system JE4, since they are all very close to each other. But, since there is removal of additive from the surface of the sample when a mar test is done, a part of the contrast in appearance of the marred region should be attributed to the presence of the scratch additive which has been removed.

This indicates that although the mold temperature affects the mar behavior significantly, the degree to which the scratch additive influences mar behavior of samples is much greater. In agreement with the visibility results, higher mold temperatures result in more additive migrating to the surface, causing slip of the mar tip and lower SCOF values and visibility.

6. CONCLUSIONS

Along with scratch and Mar tests, the physical and surface properties of the sample systems were analyzed in the form of SCOF, surface roughness, damage feature onset for scratch tests, and FTIR-ATR analysis. It should be noted that scratch and mar tests were carried out in a direction parallel to the injection molding flow direction. If the polymer molecules were to align themselves, there is a high probability that they would align themselves along the direction of flow.

From the scratch test results obtained for the High and Low MFR systems, it was found that the high melt flow rate of the system gives increasingly better scratch and mar-resistant surfaces with increasing mold temperature, owing to the molecules having more energy and less length to orient themselves on the surface and from a more crystalline surface layer. As MFR is inversely related to molecular weight, the lower MFR system has higher molecular weight distribution among its chains and therefore exhibits higher modulus and hardness. This results in a general delay in the visibility of the lower MFR system compared to the higher MFR system. The SCOF of the lower MFR system is also not very dependent on the mold temperature, which is in agreement with the above explanation, and similarly the higher MFR system shows higher scratch co-efficient of friction at lower mold temperature. Since the chain molecules align themselves in the direction of scratch, a better aligned system would have lesser resistance to scratch and mar, and would therefore exhibit lower SCOF. This is the same result obtained from the SCOF curves, supporting the theory. As expected, the lower

MFR system shows slightly better scratch resistance, and does not depend as much on the mold temperature as the higher MFR system does.

In systems JE3 and JE4, as expected, the system with scratch additive shows much improved performance than the system without. The additive's effect gets enhanced as the mold temperature was increased, since there is better migration of additive to the surface at higher mold temperatures. The onset of visibility, fish-scale and plowing got improved because of the presence of additive, which caused slip on the surface, reflected by the low SCOF, and lesser damage. However, without the scratch additive, the TPO system was by itself not heavily reliant on the mold temperature and showed no strong trend in terms of visibility or damage.

Results of Mar tests showed that reduction in surface roughness causes a darkened appearance and a lower brightness compared to the background, and an increase in surface roughness shows a higher brightness compared to the background and whitening effect. The MFR and mold temperature does not show a visibly large effect on darkening type or ironing type mar damage, but, it was observed that for roughening and more sever mar, the system with higher MFR showed better mar behavior. This can be attributed to the fact that mar behavior relies more on the surface profile and roughness of the tip and sample rather than the bulk properties such as the modulus or yield strength, which get enhanced at lower MFR.

For the JE3 and JE4 systems, the extent of additive presence on the surface of the material depends on the mold temperature and this heavily impacts mar behavior. For barrel tip tests, The system with scratch additive shows better mar behavior in terms of

visibility and friction and roughness change at higher mold temperatures. No real conclusions could be made from the visibility analysis of the cloth tip tests, since they are visible differently at different angles, show both positive and negative contrast% values on the same curve, show no differentiable trend between different mold temperatures.

Further research needs to be done roughening mar damage and darkening mar damage, and the method of analysis. There are many proposed adjustments and changes to the visibility analysis, the contrast% calculation and the imaging and observation of mar. Some of them have been tried on the course of this work and been successfully implemented whereas there are other proposed changes to the formulae which have not yet been perfected but could yield better and more accurate results.

REFERENCES

[1] Browning, R. L., et al. "Quantitative evaluation of scratch resistance of polymeric coatings based on a standardized progressive load scratch test." Surface and Coatings Technology 201.6 (2006): 2970-2976.

[2] Browning, Robert L., Han Jiang, and Hung-Jue Sue. "Scratch behavior of polymeric materials." Tribology of Polymeric Nanocomposites (2008): 354-373.

[3] Wong, M., et al. "A new test methodology for evaluating scratch resistance of polymers." Wear 256.11 (2004): 1214-1227.

[4] Kody, Robert S., and David C. Martin. "Quantitative characterization of surface deformation in polymer composites using digital image analysis." Polymer Engineering & Science 36.2 (1996): 298-304.

[5] Chu, J., L. Rumao, and B. Coleman. "Scratch and mar resistance of filled polypropylene materials." Polymer Engineering & Science 38.11 (1998): 1906-1914.

[6] Briscoe, B. J., A. Delfino, and E. Pelillo. "Single-pass pendulum scratching of poly (styrene) and poly (methylmethacrylate)." Wear 225 (1999): 319-328.

[7] Krupička, A., M. Johansson, and Anders Hult. "Use and interpretation of scratch tests on ductile polymer coatings." Progress in Organic Coatings 46.1 (2003): 32-48.

[8] Lim, G. T., et al. "An integrated approach towards the study of scratch damage of polymer." JCT Research 2.5 (2005): 361-369.

[9] Liu, Peng, et al. "Quantitative scratch visibility assessment of polymers based on Erichsen and ASTM/ISO scratch testing methodologies." Polymer Testing 30.6 (2011): 633-640.

[10] Wong, M., et al. "A new test methodology for evaluating scratch resistance of polymers." Wear 256.11 (2004): 1214-1227.

[11] Jiang, Han, Robert Browning, and Hung-Jue Sue. "Understanding of scratch-induced damage mechanisms in polymers." Polymer 50.16 (2009): 4056-4065.

[12] Goy Teck Lim. "Scratch Behavior of Polymers." Diss. Texas A&M U, 2005. Print.

[13] Kinlen, P. J., D. C. Silverman, and C. R. Jeffreys. "Corrosion protection using polyanujne coating formulations." Synthetic Metals 85.1 (1997): 1327-1332.

[14] Wang, Duhua, and Gordon P. Bierwagen. "Sol–gel coatings on metals for corrosion protection." Progress in Organic Coatings 64.4 (2009): 327-338.

[15] Tomashov, Nikon Danilovich. “Passivity and protection of metals against corrosion” Springer Science & Business Media, 2012.

[16] Burt, Gerald D., and Jr Randel Q. Little. "Detergent-dispersant lubricant additive having anti-rust and anti-wear properties." U.S. Patent No. 3,322,670. 30 May 1967.

[17] Bellezze, T., G. Roventi, and R. Fratesi. "Electrochemical study on the corrosion resistance of Cr III-based conversion layers on zinc coatings." Surface and Coatings Technology 155.2 (2002): 221-230.

[18] Jiang, Han, et al. "Quantitative evaluation of scratch visibility resistance of polymers." Applied Surface Science 256.21 (2010): 6324-6329.

[19] Ma, Yu-Fei, and Hong-Jiang Zhang. "Contrast-based image attention analysis by using fuzzy growing." Proceedings of the Eleventh ACM International Conference on Multimedia. ACM, 2003.

[20] Ginsburg, Arthur P. "Contrast sensitivity and functional vision." International Ophthalmology Clinics 43.2 (2003): 5-15.

[21] Lee, Hyuk-soo, et al. "TPO based nanocomposites. Part 1. Morphology and mechanical properties." Polymer 46.25 (2005): 11673-11689.

[22] Chum, P. Steve, and Kurt W. Swogger. "Olefin polymer technologies—history and recent progress at the Dow Chemical Company." Progress in Polymer Science 33.8 (2008): 797-819.

[23] Jiang, Han, et al. "Influence of surface roughness and contact load on friction coefficient and scratch behavior of thermoplastic olefins." Applied Surface Science 254.15 (2008): 4494-4499.

[24] Xiang, C., et al. "Scratch behavior and material property relationship in polymers." Journal of Polymer Science Part B: Polymer Physics 39.1 (2001): 47-59.

[25] Browning, Robert, et al. "Effects of acrylonitrile content and molecular weight on the scratch behavior of styrene-acrylonitrile random copolymers." Polymer Engineering & Science 51.11 (2011): 2282-2294.

[26] Pereira, Ana Paula Viana, Wander Luiz Vasconcelos, and Rodrigo Lambert Oréfice. "Novel multicomponent silicate–poly (vinyl alcohol) hybrids with controlled reactivity." Journal of Non-Crystalline Solids 273.1 (2000): 180-185.

[27] Michell, Anthony J. "Second-derivative FTIR spectra of native celluloses from Valonia and tunicin." Carbohydrate Research 241 (1993): 47-54.

[28] Retrieved from http://ocw.umb.edu/chemistry/organic-chemistry-i-lecture/lecture-links/notes92208.pdf on April 18, 2016.

[29] S. Ricordel, S. Taha, I. Cisse, G. Dorange "Heavy metals removal by adsorption onto peanut husks carbon: characterization, kinetic study and modeling" Sep. Purif. Technol., 24 (2001), pp. 389–401

[30] Srivastava, Vimal Chandra, Indra Deo Mall, and Indra Mani Mishra. "Characterization of mesoporous rice husk ash (RHA) and adsorption kinetics of metal ions from aqueous solution onto RHA." Journal of Hazardous Materials 134.1 (2006): 257-267.

[31] Yun, F., et al. "Study of structural and optical properties of nanocrystalline silicon embedded in SiO 2." Thin Solid Films 375.1 (2000): 137-141.

[32] Atalay, S., H. I. Adiguzel, and F. Atalay. "Infrared absorption study of Fe 2 O 3–CaO–SiO 2 glass ceramics." Materials Science and Engineering: A 304 (2001): 796-799.

[33] Rehman, Ihtesham, and W. Bonfield. "Characterization of hydroxyapatite and carbonated apatite by photo acoustic FTIR spectroscopy." Journal of Materials Science: Materials in Medicine 8.1 (1997): 1-4.

[34] Cantero, Guillermo, et al. "Effects of fibre treatment on wettability and mechanical behaviour of flax/polypropylene composites." Composites Science and Technology 63.9 (2003): 1247-1254.

[35] Choukourov, A., et al. "Properties of amine-containing coatings prepared by plasma polymerization." Journal of Applied Polymer Science 92.2 (2004): 979-990.

[36] Hamdi, Marouen, and Hung-Jue Sue. "Effect of color, gloss, and surface texture perception on scratch and mar visibility in polymers." Materials & Design 83 (2015): 528-535.

[37] Bremner, T., A. Rudin, and D. G. Cook. "Melt flow index values and molecular weight distributions of commercial thermoplastics." Journal of Applied Polymer Science 41.7-8 (1990): 1617-1627.

[38] Browning, Robert, et al. "Contrast-based evaluation of mar resistance of thermoplastic olefins." Tribology International 44.9 (2011): 1024-1031.

[39] Liang, J. Z., and J. N. Ness. "Investigation on the melt flow properties of polyethylene and polypropylene blends." Polymer Testing 16.4 (1997): 379-389.